



University
of Stavanger

MECHANICAL & STRUCTURAL ENGINEERING AND MATERIALS SCIENCE

MASTER'S THESIS

Study Program: Engineering Structure and material with specialization in Mechanical systems

Autumns, 2020

Open

Author: Muhammad Maaz Akhtar

.....
(author signature)

Faculty supervisor: Hirpa Gelgele Lemu
External supervisor: Øyvind Karlsen

Master thesis title: Expanding PIN system – Combined radial and axial locking system

Keywords: Bondura, pin system, preload, stress analysis, micro-asperities

Number of pages: 55
+ appendices/other: 7

Stavanger, 15.07.2020
.....
date/year

Preface

This master thesis is written in collaboration with a local company based in Bryne, Bondura Technology AS, at the Department of Mechanical and Structural Engineering and Materials Science of the University of Stavanger, to qualify for the master's degree in Engineering Structures with specialization in Mechanical Systems.

I am sincerely thankful to Professor Hirpa Gelgele Lemu, who is my faculty supervisor for this thesis. I have received continuous guidance and support from him to keep my progress in an organized flow, especially in the challenging times of lockdown due to COVID-19. This thesis could have been a hard task to achieve without his help and efforts.

I am also deeply grateful to Mr. Øyvind Karlsen, who is my external supervisor from Bondura Technology AS, for always giving me time to discuss and answer my queries regarding the product and also for providing all the necessary information related to the product.

Here, I also want to acknowledge the effort of Mr. Yaaseen Ahmad Amith, who is the lab engineer at the University of Stavanger, for helping me in the experimental work required for this thesis, in the crisis times of COVID-19.

In the end, I would like to say thanks to my family for providing support and keeping me motivated, especially my father Engr. Muhammad Saleem Akhtar.

Stavanger, 15/07/2020

Muhammad Maaz Akhtar

Executive summary

In the side by side plate joints or flange joints, the standard practice is to have a bolted connection that provides the axial clamping load as well as, avoiding any radial or rotational movement. This can be problematic since there is not much surface resistance between the bolt and the flanges which can lead to radial motion due to vibrations from heavy loading eventually failure of connection or leakage in high pressured big diameter pipe system.

Bondura Technology AS which is known for the out of the box solution for common problems of the industry comes up with a solution for this problem with there 'bondura® pin system with combined axial and radial locking system'. This pin system is in the initial design phase so, a lot of analyses are required to perform, and this thesis is a contribution to finalize and optimize the product.

This thesis is divided into two wide ranges, one part of this thesis is to analyze the different factors goes under consideration for the maximum possible preloads from the bondura® pin system and the relationship between applied torque level and preload as well as, the possible wedge effect from the conical sleeves.

And the other major focus of this thesis is the comparison between bondura® pin system and standard bolts in terms of preload capability, loss in preload due to plastic deformation of micro-asperities, and surface resistance between mating surfaces.

The preload capability is analyzed theoretically by using the relationship between applied torque and preload since the preload in the bondura® pin system comes from the application of torque to the M10x35 tightening screws.

Preload for different levels of applied torque is calculated and an experiment is designed to verify the calculated results which shows promising results with some errors. Also, ANSYS is used to simulate the stress distribution which shows the possibilities of having much more preload since the stress in most of the area is at the lower level of stress.

The bondura® pin system does provide much more surface resistance due to high mating surface area but it lacks in terms of preload capability in comparison with standard bolts. The loss in preload due to plastic deformation of micro-asperities is slightly higher for bondura® pin system than standard bolts, due to reliance on the relatively smaller size of tightening screws.

While taking different factors under consideration the best possible way to increase the preload of the bondura® pin system is by increasing the size of tightening screws as by using M12 screws the maximum possible preload is increased by 460766.95 N from M10 screws.

One of the best possible solutions for overcoming the radial and rotational movement in the flange connection is by using both bondura® pin systems and standard bolts in an optimized manner based on the individual problem as the preload comes from the standard bolts and the surface resistance from bondura® pin system. A mathematical model based on different factors involved in the design of a flange connection can be created, to have an optimized solution.

Table of Contents

Preface.....	i
Executive summary.....	ii
1 Introduction.....	1
1.1 Background.....	1
1.2 Problem definition.....	1
1.3 Limitations.....	2
1.4 Bondura Technology AS.....	2
1.4.1 Expanding PIN System – Combined radial and axial locking system....	3
1.5 Report structure.....	5
2 Literature review.....	6
2.1 Basic Definitions.....	6
2.1.1 Torque.....	6
2.1.2 Mechanical Stress.....	6
2.1.3 Mechanical strain.....	7
2.1.4 Young’s Modulus.....	7
2.2 Threaded fasteners.....	8
2.2.1 The terminology of screw thread.....	8
2.3 Bolted connections.....	9
2.4 The mechanics of Power Screws.....	9
2.5 Relating bolt tension and bolt torque.....	11
2.5.1 Torque Wrench.....	12
2.5.2 Relationship between applied torque and preload.....	12
2.6 Elastic Torsion formulas.....	13
2.7 Plastic deformation of micro-asperities.....	15
2.8 Wedges.....	17
2.9 Strain gauge.....	18
2.9.1 Wheatstone bridge.....	19
3 Theoretical Calculations.....	21
3.1 Maximum preload in bondura® pin systems.....	21
3.1.1 Maximum preload in the central pin as a function of Tightening screws strength	21
3.1.2 Maximum preload in the central pin as a function of the size of tightening screws and different number of tightening screws.....	22
3.1.3 Maximum preload in the central pin as a function of the torquing level of tightening screws	23
3.2 Loss of preload due to the reduction of micro asperities.....	24
3.3 Wedge effect from the conical sleeves.....	25
3.4 Standard bolts.....	27
3.4.1 Maximum possible preload.....	27
3.4.2 Loss of preload due to the plastic deformation of micro-asperities.....	27
3.5 Mating surface areas.....	29
3.5.1 Mating surfaces area for standard bolts and flanges.....	29
3.5.2 Mating surfaces area for bondura® pin systems and flanges.....	29
4 Experimental work.....	31
4.1 Strain gauge.....	31

4.2	Data Acquisition System	33
4.3	Application of torque.....	34
4.4	Experiment	35
5	Finite Element Analysis.....	37
5.1	Preparation for Analysis	38
5.1.1	Material.....	38
5.1.2	Coordinate System.....	38
5.1.3	Meshing	39
5.1.4	Constraints and loads	39
5.2	Solution	40
6	Discussion.....	42
6.1	Maximum possible preload	42
6.2	Torquing level of tightening screws	44
6.3	Wedge effect from conical sleeves	46
6.4	Comparison with standard bolts	47
6.5	Possibilities for bondura® pin system.....	49
6.6	Errors in the results from the experiment	50
7	Conclusion.....	52
7.1	Future work recommendations	53
8	References	54
9	Appendix	56
9.1	Appendix A: Material properties of the central pin.....	56
9.2	Appendix B: Certificate of Strain gauges.....	57
9.3	Appendix C: Calibration certificate of torque wrench.....	58
9.4	Appendix D: Drawings of bondura® pin systems.....	59
9.5	Appendix E: Stress distribution in Ø50 mm pin system at different levels of torque	61
9.6	Appendix F: Stress distribution in Ø80 mm pin system at different levels of torque.....	63
9.7	Appendix G: Excel spreadsheet for theoretical calculations	65

List of Figures

Figure 1.1: Bondura® pin system	3
Figure 1.2: Section view of Bondura® pin system with numbering of components.....	4
Figure 2.1: (a) Forces producing tension stress, (b) Forces producing compression stress, and (c) Forces producing shear stress.....	7
Figure 2.2: Change of length due to force.....	8
Figure 2.3: Terminology of screws	8
Figure 2.4: Axially loaded square-threaded power screw	9
Figure 2.5: Unrolled single screw. (a) Force diagram for raising, and (b) Force diagram for lowering	10
Figure 2.6: Forces applied on a thread which indicating the normal force increase with increment in thread angle.....	11
Figure 2.7: Collar bearing employed between stationary and rotating member.....	12
Figure 2.8: Distribution of shear stress in a cross section of shaft	14
Figure 2.9: Distribution of stress in bolted connection	16
Figure 2.10: Wedge application	17
Figure 2.11: Free Body Diagram of wedge application	17
Figure 2.12: Geometrical representation of forces from wedge application	18
Figure 2.13: Pattern of strain gauge	18
Figure 2.14: Wheatstone bridge	19
Figure 2.15: Three configurations of Wheatstone bridge for measuring strain.....	20
Figure 3.1: Section of the mating surfaces between conical sleeve and nut plate.....	25
Figure 3.2: Graphical representation of the forces	26
Figure 3.3: Reaction forces from wedge action of conical sleeve.....	26
Figure 3.4: Highlighted mating surfaces between standard bolt and flanges	29
Figure 3.5: Highlighted mating surfaces between bondura® pin system and flanges	29
Figure 4.1: Test jig instead of complete flange	31
Figure 4.2: Locations of Strain gauges on central pin.....	32
Figure 4.3: Active strain gauges on Ø50mm central pin.....	32
Figure 4.4: Dummy strain gauges	33
Figure 4.5: Basic type of Spider8 with 600 Hz	33
Figure 4.6: Real time data display for Ø50mm pin system.....	34
Figure 4.7: Dial of USAG torque wrench indicating range from 40 to 200 Nm.....	34
Figure 4.8: Application of torque using USAG torque wrench.....	34
Figure 4.9: Sequence of different parts of bondura® pin systems	35
Figure 4.10: Broken M10x35 tightening screws for both bondura® pin systems.....	35
Figure 5.1: Bondura® material in the library	38
Figure 5.2: Coordinate system for 50mm central pin.....	39
Figure 5.3: Meshed view of 50mm central pin.....	39
Figure 5.4: Fixed support on 50mm central pin	40
Figure 5.5: Load applied on the 50mm central pin.....	40
Figure 5.6: Normal stress along x-axis for 50mm central pin	41
Figure 6.1: Relationship between strength of M10x35 tightening bolts and preload in pin.....	43
Figure 6.2: Relationship between screw sizes of 16.9 strength class and preload	43
Figure 6.3: Relationship between number of tightening screws and preload.....	43
Figure 6.4: Relationship between torque level and calculated preload for M10x35-16.9 tightening screws	45

Figure 6.5: Relationship between applied torque level and measured preload from experiment for both pin systems.....	45
Figure 6.6: Relationship between torque level and average normal stress from finite element analysis for both pin systems.....	45
Figure 6.7: Stress distribution at 157.08 Nm torque in Ø50 mm pin system	46
Figure 6.8: Stress distribution at 157.08 Nm torque in Ø80 mm pin system	46
Figure 6.9: Component of reaction force R_2 from wedge effect of conical sleeve.....	48
Figure 6.10: Fixture used with torque wrench.....	51
Figure 9.1: Certificate for strain gauges	57
Figure 9.2: Calibration certificate of torque wrench	58
Figure 9.3: Drawing for Ø50 mm pin system.....	59
Figure 9.4: Drawing for Ø80 mm pin system.....	60
Figure 9.5: Stress distribution at 40 Nm torque in Ø50 mm pin system	61
Figure 9.6: Stress distribution at 60 Nm torque in Ø50 mm pin system	61
Figure 9.7: Stress distribution at 80 Nm torque in Ø50 mm pin system	61
Figure 9.8: Stress distribution at 100 Nm torque in Ø50 mm pin system	62
Figure 9.9: Stress distribution at 120 Nm torque in Ø50 mm pin system	62
Figure 9.10: Stress distribution at 140 Nm torque in Ø50 mm pin system	62
Figure 9.11: Stress distribution at 40 Nm torque in Ø80 mm pin system	63
Figure 9.12: Stress distribution at 60 Nm torque in Ø80 mm pin system	63
Figure 9.13: Stress distribution at 80 Nm torque in Ø80 mm pin system	63
Figure 9.14: Stress distribution at 100 Nm torque in Ø80 mm pin system	64
Figure 9.15: Stress distribution at 120 Nm torque in Ø80 mm pin system	64
Figure 9.16: Stress distribution at 140 Nm torque in Ø80 mm pin system	64
Figure 9.17: Calculations for different strength classes, sizes and number of tightening screws	65
Figure 9.18: Calculations for preload, normal stress and normal strain at different levels of torque	65
Figure 9.19: Calculations for loss in preload for bondura® pin systems and standard bolts	66
Figure 9.20: Wedge calculations for conical sleeves	66
Figure 9.21: Preload calculations for standard bolts	66
Figure 9.22: Calculations for mating surface area of both type of fasteners.....	66

List of Tables

Table 1.1: Components of bondura® pin system	4
Table 2.1: Torque coefficients for different bolt conditions	13
Table 3.1: Number of tightening screw in both bondura® pin systems	21
Table 3.2: Preload per screw and maximum preload in both pin systems for different strength classes of tightening screws	22
Table 3.3: Preload per bolt and maximum preload in both pin systems for different sizes of tightening bolts	22
Table 3.4: Maximum preload for different number of tightening screw	23
Table 3.5: Maximum preload for different levels of torque for both bondura® pin systems	24
Table 3.6: Average normal stresses and strains for different levels of torque	24
Table 3.7: Loss in preload and remaining preload in both pin systems	25
Table 3.8: Numerical results of the wedge effect of conical sleeve for both pins.....	28
Table 3.9: Applied torque and maximum preload for different property classes of the M50 bolt	28
Table 3.10: Applied torque and maximum preload for different property classes of the M80 bolt	28
Table 3.11: Mating surface areas between M50 and M80 bolt and surface of flanges	30
Table 3.12: Mating surface areas between Ø50 mm and Ø80 mm bondura® pin system and the surface of flanges	30
Table 4.1: Measured strains due to applied torque for both pin systems	36
Table 4.2: Stresses from measured strains for both pin systems	36
Table 4.3: Effect of conical sleeves in terms of measured strains.....	36
Table 5.1: Average normal stress and strain for applied torque and preload in 50 mm central pin	40
Table 5.2: Average normal stress and strain for applied torque and preload in 80 mm central pin	41
Table 6.1: Stress and preload for both bondura® pin systems calculated from measured strain	44
Table 6.2: Stress in central pin due to the wedge effect from calculations and experiment.....	47
Table 6.3: Difference between preloads of bondura® pin systems and standard bolts.....	48
Table 6.4: Required number of fasteners for the desired preload	48
Table 6.5: Loss in preload for bondura® pin systems and standard bolts.....	48
Table 6.6: Mating surface area for different types of fasteners.....	48
Table 6.7: Error between measured and calculated values for Ø50 mm pin system.....	50
Table 6.8: Error between measured and calculated values for Ø80 mm pin system.....	50
Table 9.1: Material properties of the central pin	56

1 Introduction

1.1 Background

In the side by side connections of plates and flanges to avoid any radial and axial movement several nuts and bolts are used. In this conventional practice, nuts and bolts are serving to prevent both axial and radial movement of flanges as, the clamping force is applied by the torquing the nuts which prevent any axial movement and, the radial movements are designed to be avoided by the surface resistance between the mating surfaces of nuts and bolt and the surface of flanges.

The drawback of this conventional practice comes from the total reliance on avoiding the radial and rotational movements on the mating surfaces of nuts and bolts with flanges. Minor radial movements can lead to the total failure of connection or in case of the pressurized big diameter pipe system, leakage could occur because in flange connections there are always small vibrations because of exposure to heavy loads. These vibrations reduce the surface friction by decreasing the size of surface micro-asperities and eventually, it will cause a reduction in the axial load which leads to the failure of connection.

In the flange-bolted joint, there is tolerance between the diameter of the bolt and the bolt hole diameter of the flange for easy installation. When the clamping force of the bolted joint is decreased due to vibrations, this difference in sizes leads to wear and tear of the bore of flanges due to the radial and rotational movements of bolts. This problem can be avoided by eliminating the tolerance but, that will damage the bolt hole of flanges while sliding in the bolt.

Therefore, to avoid this damage, there is a solution in practice, the bolt is frozen before sliding in as this will reduce the bolt diameter and by that increase the installation tolerance. This solution also has a drawback, while disassembly or maintenance, the bolt cannot be taken out easily, but it needs to be removed by using the torch cutting. This will damage the bolt hole diameter of flanges which has to be repaired therefore, it has a high associated cost.

Bondura Technology AS has an impressive and innovative solution for this rather complicated problem with its “Expanding PIN System – Combined radial and axial locking system” for which the company has also got Norwegian patent approved. This pin system is in the design phase but, with full potential to overcome this problem as this pin system is equipped with two tapered conical sleeves to avoid the radial movements.

With the collaboration of Bondura Technology AS, at the University of Stavanger, we will try to examine the different prospects of two bondura® expanding pin systems, Ø50mm and Ø80mm, to attain the Master’s degree in Engineering Structure and Materials with specialization in Mechanical System.

1.2 Problem definition

Bondura® pin system with combined axial and radial locking system is in its initial phase of testing and verification so, a lot of theoretical, numerical, and experimental analyses are

required to finalize and optimize the product. In this section, the main objectives of this thesis are defined which are performed throughout the semester.

Before going further it is important to understand the terminology used in this thesis, the term ‘bondura® pin system’ refers to the full assembly of bondura® expanding pin system – combined radial and axial locking system, ‘pin’ refers to central load-bearing pin and ‘tightening screws’ refers to M10 bolts which are further explained in Sub-section 1.4.1.

There are four main objectives of this thesis,

1. Maximum possible preload in both of the pins of the bondura® pin system as a function of:
 - Tightening screw strengths which are additionally hardened
 - Number and size of the tightening screws
 - Torquing level of tightening screws
2. Analyzing the loss of preload in pins due to the reduction of micro-asperities as well as, the wedge effect from the conical sleeves on the preload
3. For the feasibility study of the bondura® pin system, it is important to make a comparison with the standard bolts. First, there is a comparison between one bondura® pin system and one standard bolt. After that for an assumed situation a comparison between the required numbers of bondura® pin system and standard bolts. This comparison includes the preload as a function of torquing level and also loss in preload as a function of reduction of asperities
4. Value of having sleeves to prevent torsional rotation instead of shear resistance.

Theoretical work is verified by experimental and numerical analysis. For the experimental work on both Ø50 mm and Ø80 mm PINs, strain gauges are used for measuring the strain for different levels of torque as well as the effect of tightening of expanding sleeves. For numerical work, AutoDesk Inventor and ANSYS software are used.

1.3 Limitations

The project is limited to only two sizes of bondura® pin systems, Ø50mm and Ø80mm, and this project mainly covers the preload in the pins and factors affecting this preload. This thesis does not provide any information about the design of the pin as all the designing is done by Bondura Technology AS. Other limitations throughout the project are:

- Limited access to university due to COVID-19
- Problems while pasting the strain gauges, which is to be discussed later in this thesis
- Limitations in Finite Element Analysis due to student licenses of Softwares

1.4 Bondura Technology AS

The company was founded in 1986 by Mr. Aarre under the name of Bolt Norge AS and got its first patent for a lubrication-free pin the same year. A prototype was made in 1991 and with the permission of a local contractor this prototype was tested on an excavator which showed long-term successful results and the bondura® pivot pin was born. The same year big companies like

Esso Norway and Exxon Group started to use bondura® pin in offshore operations under the “maintenance free” innovative project and Bolt Norge AS got DNV GL Type approval. In 1992, design for bondura® pin was patented.

After this company worked with Statoil and in 1993, the bondura® pin was recognized as “proven technology” by Statoil and Norwegian Veritas. In 1995 Bolt Norge AS was merged with Serigstad. In the time of two years after joining the BMC Group in 2005, the company started its own production in 2007 and entered in US market in 2011. Bolt Norge changed its name to Bondura Technology AS in 2013 and entered in the Asian market. Recently in 2014, bondura® also got ABS PDA [1].

1.4.1 Expanding PIN System – Combined radial and axial locking system

Bondura Technology AS was started from an out of the box thinking and innovating a solution for a common problem in the industrial sector. It is continuing its legacy and working on a solution for the problem in the bolted connection between two flanges or plates. “Expanding PIN System – Combined radial and axial locking system” is innovatively designed by Bondura Technology AS to overcome the problems which are associated with standard nut and bolt, used for the bolted connection between two plates or flanges.

As illustrated in Figure 1.2, which is the section view of Figure 1.1, bondura® pin system consists of a total of seven different components numbered as:

1. Central pin
2. Coned nuts
3. M10x35 tightening screws
4. Conical Sleeves
5. End plates
6. M10x60 tightening screws
7. Shims

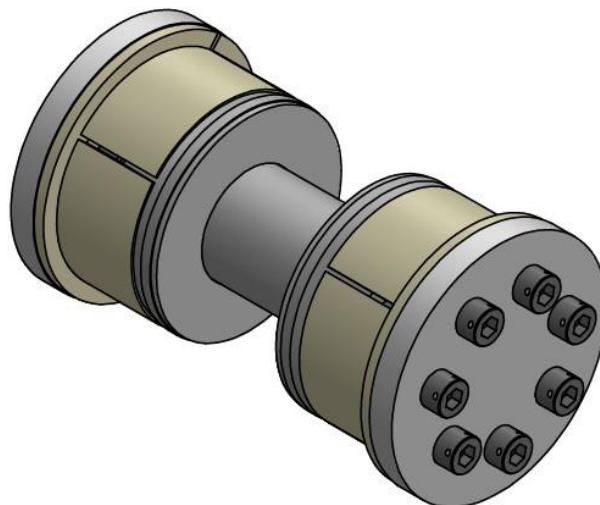


Figure 1.1: Bondura® pin system

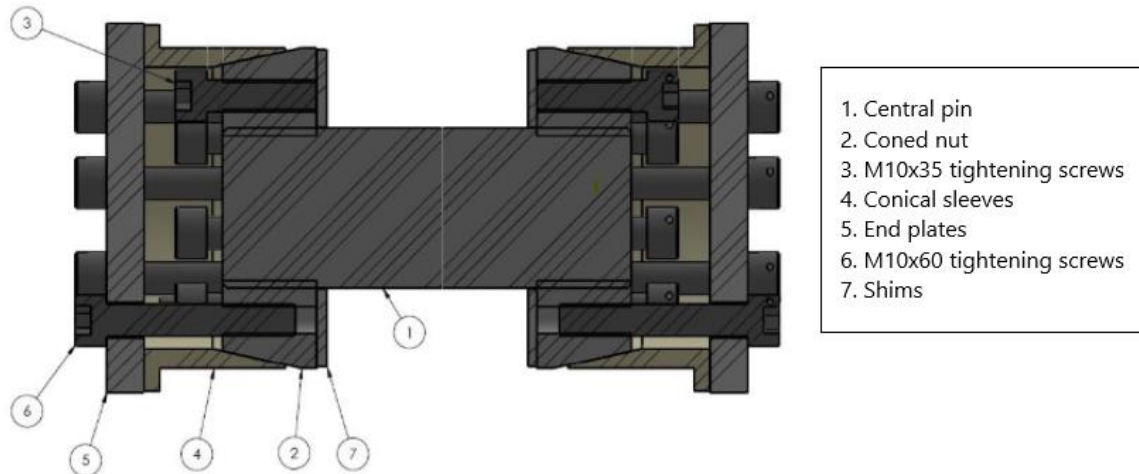


Figure 1.2: Section view of Bondura® pin system with numbering of components

Components of the bondura® pin system are further explained in Table 1.1 individually.

Table 1.1: Components of bondura® pin system

Sr. no.	Component	Diagram	Description
1	Central pin		It is the central component of the pin system with external threads on both sides for coned nuts. This pin goes under stress while preloading.
2	Coned nut		There are two coned nuts in the pin system which are screwed on both sides of the central pin. It has a number of holes with internal threads equal to the sum of the number of both tightening screws.
3	Conical Sleeves		It is the main component of the pin system with the purpose of eliminating the radial and rotational movements. It has three limited cuts and one cut through all.
4	Shim		To avoid the damage of the impact of tightening screws on the surface of the flanges these shims are used on both sides of the central pin. These shims are also further hardened.
5	End plate		To push and keep the conical sleeves in the assembly these end plates are used on both sides of the pin system. It has go-through unthreaded holes for M10x60 tightening screws.

The number of M10x35 and M10x60 tightening screws depends on the diameter of the central pin. The Ø50 mm pin system has fourteen M10x35 tightening screws as well as fourteen

M10x60 tightening screws and in Ø80 mm pin system there are twenty-four M10x35 tightening screws but only twelve M10x60 tightening screws.

First, the pin which has threads on both ends installed in the bolt hole of flanges, and then shims are inserted on both sides. The shims are hardened to shield the flange surface from the application of the direct point load of M10x35 tightening screws. Conical nuts are screwed on both sides of the central pin and here preload is applied by M10x35 tightening screws from both sides as they tightened up in conical nuts.

To avoid the radial movements of the bolt system, conical sleeves are used to eliminate the radial tolerance between the bondura® pin system and the flange surface. End plates are used to force the conical sleeves to slide inside where the load is applied using M10x60 tightening screws.

1.5 Report structure

Here in this section, a brief description of this report is provided to make it easier for the reader. This thesis is comprised of eight chapters and all the discussions on the results from theoretical, experimental, and Finite Element analysis are combined in Chapter 6 with the justifications on the differences between these results.

After this first chapter, there is a ‘Literature review’ chapter providing the necessary knowledge required for the work in this thesis which covers mainly the introduction of some basic definitions, basics of threaded fasteners, the relationship between preload and applied torque, elastic torsion formulas, plastic deformation of micro-asperities, wedges, as well as the introduction of strain gauges.

The third chapter of this thesis covers the procedures and numerical results from the theoretical calculations which are performed to make the feasibility report of the bondura® pin systems as well as comparison with the standard bolts. This chapter covers mainly the maximum possible preload in the bondura® pin systems, loss in preload due to plastic deformation of micro-asperities, wedge effect from the conical sleeve, the preload calculations as well the loss in preload for standard bolts and at the end mating surface areas between flanges and both bondura® pin system, and standard bolts. All these calculations are done on Microsoft Excel and the screenshots of the spreadsheet are attached in Appendix G.

In the fourth chapter of this thesis, the experimental work is described in detail which was done to verify the preload in the central pin at different levels of torque.

The fifth chapter covers the detailed description of Finite Element analysis which was performed to find the stress distribution in the central pin.

The most important chapter of this thesis is Chapter 6, which contains all the discussions made on the results from the previous three chapters.

Finally, in the last chapter, this thesis is concluded with some recommendations for future work.

2 Literature review

In this chapter, a theoretical background is established which is important to carry out the different tasks required to achieve the objectives. This chapter covers the introduction of the basic mechanical phenomenon, introductions to threaded fasteners, mechanics of power screws, the relationship between bolt tension and bolt torque, elastic torsion formulas, plastic deformation of micro-asperities as well as introduction to strain gauges and their working principle and wedges.

2.1 Basic Definitions

This subsection covers the introduction of some basic concepts which are important in mechanical design problems.

2.1.1 Torque

Torque is a vector product of applied force, \mathbf{F} , and the moment arm, \mathbf{r} [2].

$$\mathbf{T} = \mathbf{F} \times \mathbf{r} \quad (2 - 1)$$

The moment arm is the perpendicular distance between the point of application and the direction of the force.

2.1.2 Mechanical Stress

Mechanical stress is the magnitude of applied forces on a unit area. It further classified based on the application of force as Normal stress, Shear stress, Bending stress, and so on.

2.1.2.1 Normal Stress

Mechanical stress which is produced by the application of forces perpendicular to the cross-section of the member in the same axis is called normal stress. Based on the direction of applied forces the normal stress is further divided into tension and compression stresses as shown in Figure 2.1(a) and (b) respectively. When the forces are applied in the opposite direction that will produce an elongation in the member, this stress is called tension stress and it is represented by a positive sign with the magnitude of stress. Whereas, if both forces are applied in the direction of the centre of the member that will compress the member, this stress is called compressive stress and it is represented by a negative sign with the magnitude of stress.

The equation to calculate the average normal stress is:

$$\sigma = \frac{F}{A} \quad (2 - 2)$$

Measuring units for stress, according to the SI system is pascals [Pa] which is equal to N/m^2 .

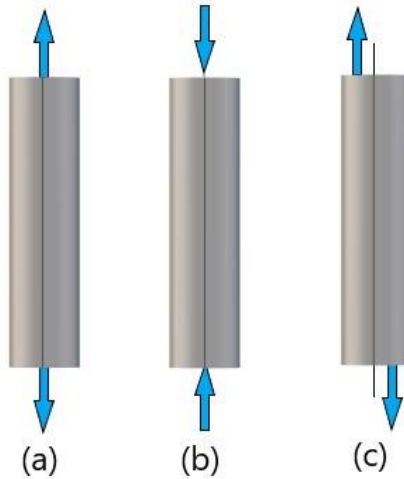


Figure 2.1: (a) Forces producing tension stress, (b) Forces producing compression stress, and (c) Forces producing shear stress

2.1.2.2 Shear stress

Mechanical stress which is produced because of the application of forces parallel to the cross-section of the member is called shear stress. In shear stress, forces are being applied in the opposite direction but contrary to tension stress both forces do not pass through the same axis as shown in Figure 2.1(c). Shear stress for 2D applications is calculated by using the normal stresses as:

$$\tau = \frac{\sigma_1 - \sigma_2}{2} \quad (2 - 3)$$

where, σ_1 is maximum and σ_2 is minimum normal stress.

2.1.3 Mechanical strain

Mechanical strain is used to quantify the change of a parameter to the original value due to external effects. If a force is applied and the parameter is length, then the equation to calculate the strain is:

$$\varepsilon = \frac{l - l_0}{l_0} \quad (2 - 4)$$

Where, l_0 is the original length and the l is new length, as shown in Figure 2.2.

Like normal stresses, the strain can also be negative or positive based on the elongation or compression of the member.

2.1.4 Young's Modulus

It is the mechanical property which establishes the relationship between stress and strain as,

$$\sigma = E\varepsilon \quad (2 - 5)$$



Figure 2.2: Change of length due to force

where E is Young's modulus.

2.2 Threaded fasteners

The most commonly and widely used mean for connecting different components in machines and structures is the threaded fasteners because it offers many distinct advantages. Threaded fasteners are readily available in the market with different mechanical and geometrical properties. They can be installed safely by hand or power tools. In maintenance, it is also easy to remove and replace if required. One of the big advantages of threaded fasteners that, they can be used to connect components of the same or different materials.

The basic system of threaded fastener consists of a male element, which has external threads like bolt, stud, or screw. And a mating female element, which has internal threads like nut or tapped hole. Manufacturing of threaded fastener depends on its size as small fasteners are made by using cutting tools such as dies for external threads and taps for internal threads. Relatively large fasteners are manufactured by different lathe operations or rolling process.

2.2.1 The terminology of screw thread

According to Collins, the terminology of threaded fasteners and power screw is similar which is illustrated in Figure 2.3 [3], the *Major diameter*, d , is the largest diameter of the thread and the smallest diameter or the root diameter of the thread is called *Minor diameter*, d_r . Whereas, the *Pitch diameter*, d_p , is the imaginary cylinder at a point where the distance between major and minor diameter is equal and it is also referred to as the effective diameter.

Pitch, p , is the axial distance between any two correspondent points on the neighbouring thread and another important term is *lead* which is the total axial displacement for one rotation of nut.

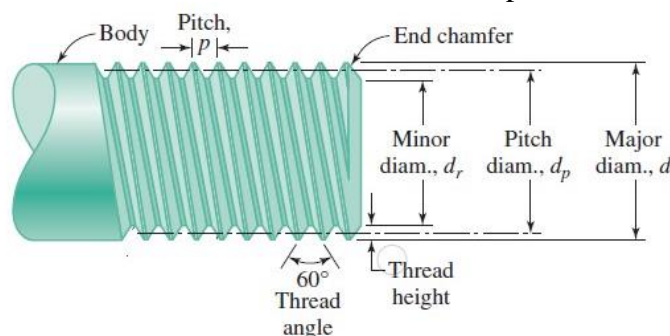


Figure 2.3: Terminology of screws

2.3 Bolted connections

Most of the machine components are manufactured as split parts but they must work as a unit when operating, which is achieved by using bolted connections (BCs). A strong pressure, which should be enough to avoid any slippage or separation in the connection, is applied to the connected parts to give it the required strength and rigidity.

It is possible to have bolted connections loaded both in shear and in tension. If the friction between flanges endures the shear load it has zero influence on the resistance to tension load. With this advantage, calculations for tension load can be made without considering the shear load. Contrary to that, bending and tension loads do change the pressure on the mating parts so, for the calculations of shear strength they must be considered.

There are several steps for the calculation of strength in bolted connections

- Find the most loaded bolt
- Study the dependence between stress and the load
- Determine the safety factor for stationary as well as cyclic load

2.4 The mechanics of Power Screws

Power screws are used to transfer angular motion to linear motion and, mostly to transmit power. Figure 2.4 shows the square-threaded power screw which is loaded by axial compressive force F and torque is required to raise and lower this load [4].

To get the expression for the required torque, imagine an unrolled single thread for exactly a single turn as shown in Figure 2.5 [4]. The angle ' λ ' is the lead angle of thread, ' f ' is the coefficient of friction and ' N ' is the normal force. ' P_R ' is the required load to raise and ' P_L ' is the load that acts to lower. By assuming that the system is in equilibrium, for raising from Figure 2.5(a):

$$\begin{aligned}\sum F_x &= P_R - N \sin \lambda - f N \cos \lambda = 0 \\ \sum F_y &= -F - f N \sin \lambda + N \cos \lambda = 0\end{aligned}\tag{a}$$

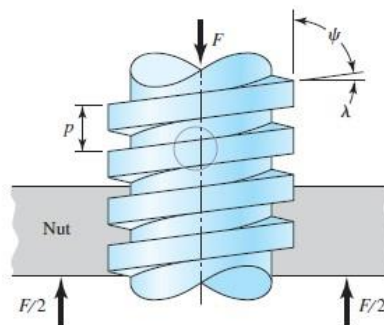


Figure 2.4: Axially loaded square-threaded power screw

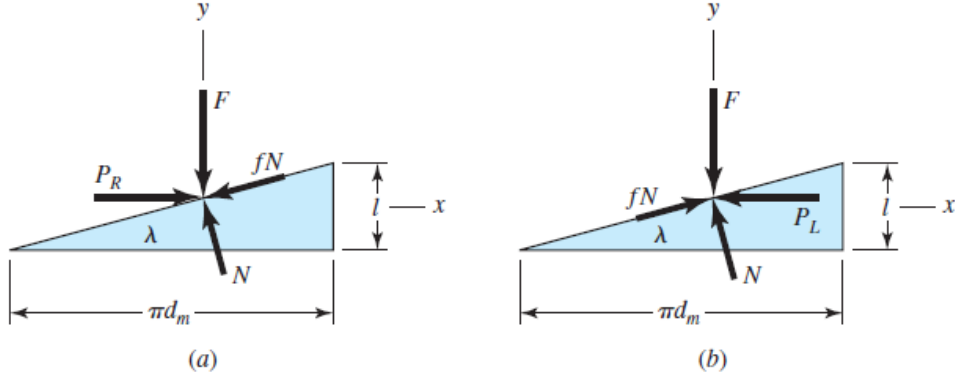


Figure 2.5: Unrolled single screw. (a) Force diagram for raising, and (b) Force diagram for lowering

Similarly, for lowering from Figure 2.5(b):

$$\begin{aligned}\sum F_x &= -P_L - N\sin\lambda + fN\cos\lambda = 0 \\ \sum F_y &= -F + fN\sin\lambda + N\cos\lambda = 0\end{aligned}\quad (b)$$

Since load P is the major focus here and the normal force N is not the main interest so, by eliminating N from the above equations and solving the results, it gives for raising:

$$P_R = \frac{F(\sin\lambda + f\cos\lambda)}{\cos\lambda - f\sin\lambda}\quad (c)$$

And, for lowering:

$$P_L = \frac{F(f\cos\lambda - \sin\lambda)}{\cos\lambda + f\sin\lambda}\quad (d)$$

By dividing the denominator and numerator of these equations with $\cos\lambda$ and using the relation, $\lambda = l/\pi d_m$. Equations (c) and (d) becomes, respectively,

$$P_R = \frac{F[(l/\pi d_m) + f]}{1 - (fl/\pi d_m)}\quad (e)$$

$$P_L = \frac{F[f - (l/\pi d_m)]}{1 + (fl/\pi d_m)}\quad (f)$$

As mentioned before, torque is the product of the applied force and radius of the arm. Therefore, the required torque is the product of load P and half of the mean diameter d_m . For raising, the torque T_R is required for two purposes: to raise the load and to overcome the thread friction, as:

$$T_R = \frac{F d_m}{2} \left(\frac{l + \pi f d_m}{\pi d_m - fl} \right)\quad (2-6)$$

and, for lowering the torque T_L is:

$$T_L = \frac{F d_m}{2} \left(\frac{\pi f d_m - l}{\pi d_m + fl} \right)\quad (2-7)$$

This is the torque which acts to overcome the friction while lowering the load. In some specific cases, it is possible that the friction is considerably low or the lead is large enough that the load

will lower itself by spinning the screw without any external input. In such cases, the torque T_L is zero or negative. But if Equation (2-7) gives a positive value than the screw is in self-locking. Therefore, the condition for self-locking is $\pi f d_m > l$. Now, by dividing both sides of inequality with πd_m , the result is $f > \tan \lambda$.

From this relation, it can be assumed that the self-locking is obtained whenever the coefficient of friction is greater than the tangent of the lead angle of the thread.

Until this point, the equations which are developed are for square threads, where the normal thread load is parallel to the screw axis. In ACME and other threads, the load is inclined to the axis because of the lead angle and the thread angle. As, the lead angles are very small, so this inclination can be ignored and only the effect of thread angle should be considered.

Figure 2.6 is indicating that the thread angle is increasing the frictional force due to the wedging action of the threads [4]. To use the torque equation of square threads it is required to divide every frictional term by $\cos \alpha$, which yields

$$T_R = \frac{F d_m}{2} \left(\frac{l + \pi f d_m \sec \alpha}{\pi d_m - f l \sec \alpha} \right) \quad (2 - 8)$$

In the case of axially loaded screws, a collar bearing is required to be employed between stationary and rotating members, as shown in Figure 2.7, to carry the axial component, therefore, the third component of torque is required [4]. If d_c is mean diameter of collar and f_c is the coefficient of friction for collar than the required torque is:

$$T_c = \frac{F f_c d_c}{2} \quad (2 - 9)$$

2.5 Relating bolt tension and bolt torque

If it is possible to measure the overall length of the bolt with a micrometer after assembling than by using the relation $\delta = F_i l / (AE)$, bolt elongation for the preload F_i would be easily computed. Then the desired preload can be achieved correctly just by elongating the bolt to a

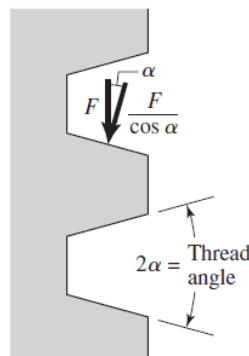


Figure 2.6: Forces applied on a thread which indicating the normal force increase with increment in thread angle

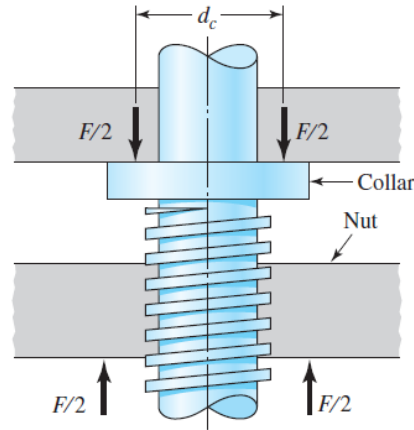


Figure 2.7: Collar bearing employed between stationary and rotating member

a certain distance. But this approach is impractical since in most of the assemblies threaded end is in the blind hole. Alternatively, the torque wrench is used to ensure the specified amount of preload.

2.5.1 Torque Wrench

Applied torque is indicated on torque wrenches with the built-in dial, and to make sure the specific torque there are two types of methods in practice: pneumatic-impact wrenching or the turn-of-the-nut method [5].

In pneumatic-impact wrenching, the wrench stalls as the required amount of torque is achieved by adjusting the air pressure, or in some other wrenches, at the desired torque the air shuts off automatically.

For the turn-of-the-nut method, it is important to understand the meaning of the snug-tight. When the tightness is achieved by using the few impacts of impact wrenching or by ordinary wrench with the full effort of a person, that condition is called snug-tight. In the turn-of-the-nut method, every turning after the snug-tight develops useful tension in bolt. In this method, it is required to compute the fractional number of turns from the snug-tight condition to achieve the required preload. In some new generations of the torque wrench of this type also stalls at the desired torque.

2.5.2 Relationship between applied torque and preload

According to Budynas and Nisbett, the relationship between the applied torque and preload can be estimated by using the torque equations from the power screw even though, the coefficient of friction may vary widely [4]. So, by using the Equation (2-8) and (2-9),

$$T = \frac{F_i d_m}{2} \left(\frac{l + \pi f d_m \sec \alpha}{\pi d_m - f l \sec \alpha} \right) + \frac{F_i f_c d_c}{2} \quad (a)$$

As $\tan \lambda = l / \pi d_m$ so, by dividing the denominator and numerator of the first term by πd_m , the Equation (a) becomes,

$$T = \frac{F_i d_m}{2} \left(\frac{\tan \lambda + f \sec \alpha}{1 - f \tan \lambda \sec \alpha} \right) + \frac{F_i f_c d_c}{2} \quad (b)$$

Generally, the diameter of the washer is equal to one and a half times the nominal diameter. Hence, the mean diameter of the collar is: $d_c = (d + 1.5d)/2 = 1.25d$. by inserting this in Equation (b) and after rearranging it becomes,

$$T = \left[\left(\frac{d_m}{2d} \right) \left(\frac{\tan \lambda + f \sec \alpha}{1 - f \tan \lambda \sec \alpha} \right) + 0.625 f_c \right] F_i d \quad (c)$$

The term in the square bracket can be defined as torque coefficient K, so

$$K = \left(\frac{d_m}{2d} \right) \left(\frac{\tan \lambda + f \sec \alpha}{1 - f \tan \lambda \sec \alpha} \right) + 0.625 f_c \quad (2 - 10)$$

Therefore, Equation (c) becomes,

$$T = K F_i d \quad (2 - 11)$$

According to Shigley, the value of K is an experimental estimation and provided for different conditions in Table 2.1.

2.6 Elastic Torsion formulas

According to Beer-Johnston, at the distance ρ from the shaft's axis, the shearing stress can be expressed as [6],

$$\gamma = \left(\frac{\rho}{c} \right) \gamma_{max} \quad (a)$$

where c is the radius of the circular shaft.

And from Hooke's law, for shearing strain and stress,

$$\tau = G \gamma \quad (b)$$

Table 2.1: Torque coefficients for different bolt conditions

Bolt condition	K
Nonplated, back finish	0.30
Zinc-plated	0.20
Lubricated	0.18
Cadmium-plated	0.16
With Bowman Anti-Seize	0.12
With Bowman-Grip nuts	0.09

where G is the modulus of rigidity.

Multiplying the modulus of rigidity on both sides of Equation (a) gives,

$$\gamma G = \left(\frac{\rho}{c}\right) G \gamma_{max} \quad (c)$$

Now, using the Equation (b) results in,

$$\tau = \left(\frac{\rho}{c}\right) \tau_{max} \quad (d)$$

This shearing stress increases from the centre of the shaft towards the edge and this distribution of shear stress as shown in Figure 2.8 [6]. The magnitude of torque T is equal to the sum of all the moments of the elementary forces applied on any cross-section of the circular shaft:

$$T = \int \rho(\tau dA) \quad (e)$$

Substituting the expression of τ from Equation (d) to (c) gives

$$T = \frac{\tau_{max}}{c} \int \rho^2 dA \quad (f)$$

The last term of Equation (f) is equal to the polar moment of inertia of the cross-section so the relationship between torque and maximum shear stress can be simplified as,

$$T = \frac{\tau_{max}}{c} J \quad (2 - 12)$$

Or,

$$\tau_{max} = \frac{Tc}{J} \quad (2 - 13)$$

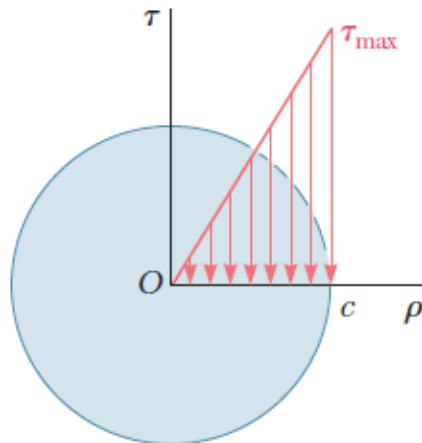


Figure 2.8: Distribution of shear stress in a cross section of shaft

2.7 Plastic deformation of micro-asperities

Plastic deformation in fasteners starts with the initial application of preload and with the time under the effect of micromovements and high pressure the micro asperities continue to reduce and eventually fasteners start to lose the part of preload [5]. To predict the loss of preload it is important to first calculate the elastic deformation of different connection members which is quite challenging by using the traditional methods.

Boris uses Briger's recommendation for this purpose. According to Briger's recommendations, first, calculate the compliance of connection members and then multiply the tightening force with the compliance which gives the elastic elongation.

Compliance of bolt is the total summation of compliances of thread, bolt head, and bolt shank.

Compliance of thread can be calculated by:

$$\lambda_t = \frac{0.85}{dE} \quad (2 - 14)$$

where d is the diameter of the thread.

For compliance of the bolt head:

$$\lambda_h = \frac{0.15}{hE} \quad (2 - 15)$$

where h is the height of the bolt head.

And finally compliance of bolt shank:

$$\lambda_{sh} = \frac{L}{EA_s} \quad (2 - 16)$$

where L is the length of bolt shank which is between the bolt head and bearing surface of the nut, and A_s is the cross-sectional area of the shank.

Hence, the compliance of the bolt is:

$$\lambda_b = \lambda_t + \lambda_h + \lambda_{sh} \quad (2 - 17)$$

Now, the elastic elongation of the bolt can be calculated by using the following equation:

$$\Delta_b = F_t \lambda_b \quad (2 - 18)$$

The second part of the bolted connection is the flange and to calculate the compliance of the flanges the following equation is used:

$$\lambda_f = \frac{2}{E_f \pi d_0 \tan \alpha} \ln \frac{(d_1 + d_0)(d_1 + L \tan \alpha - d_0)}{(d_1 - d_0)(d_1 + L \tan \alpha + d_0)} \quad (2 - 19)$$

where, d_1 is the diameter of the bolt head, and d_0 is the diameter of the bolt as shown in Figure 2.9 [5].

Here angle ' α ' is used to determine the cone of pressure and Boris recommends using the value between the range of 22° and 27° . The error because of this assumption is negligible in normal cases but for important cases, it should be calculated either by experimentally or by using FEM.

Similarly, to calculate the elastic deformation of the flanges following equation can be used:

$$\Delta_f = F_t \lambda_f \quad (2 - 20)$$

Now, the summation of both Equations (2-18 & 2-20) will give the total elastic deformation:

$$\Delta = \Delta_b + \Delta_f \quad (2 - 21)$$

The ratio of reduction of the initial elastic deformation (R_{ed}) can be calculated by using the following equation:

$$R_{ed} = \frac{\Delta'}{\Delta} \quad (2 - 22)$$

where, Δ' is a decrease in the elastic deformation which can be calculated as:

$$\Delta' = 2 \times R_p \times h_{ma} \times CS \quad (2 - 23)$$

where, R_p is the ratio of plastic deformation of micro-asperities by height, h_{ma} is mean height of micro-asperities, and CS is pairs of contacting surfaces of the bolted connection

Finally, the loss of preload due to the reduction of asperities can be calculated by the product of the ratio of reduction of the initial elastic deformation and the initial preload as,

$$F_{lost} = R_{ed} \times F_t \quad (2 - 24)$$

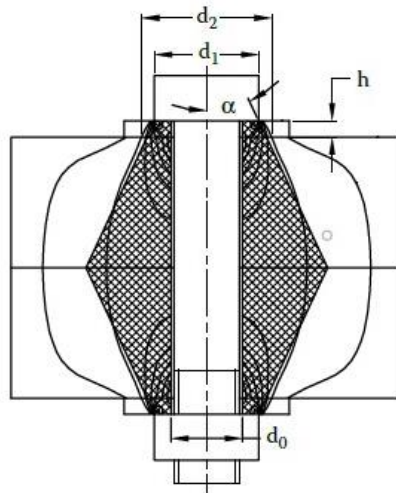


Figure 2.9: Distribution of stress in bolted connection

2.8 Wedges

Wedges are one of the simplest but very useful machines to lift heavy objects or to fix the position of a body. Friction plays a very important role in the functioning of wedges as, the resultant force inclined to normal of the surface by an angle, depending on the coefficient of friction $\mu = \tan\phi$. There is friction force against the motion of wedge, which is the component of resultant force along the surface.

The solution for wedges problems come easily from graphical methods [2]. In Figure 2.10 a wedge is slide under the mass to produce a lift force where the inclination angle of the wedge is α and force P is applied on the wedge. To make the calculations simple there is an assumption that, the mass of wedge is relatively very small therefore it can be neglected. Figure 2.11 is showing a free body diagram for the problem in which a reaction force, R_2 , is applied on both mating surface which is inclined to normal of the surface by the angle ϕ which, comes from the coefficient of friction. The weight of the body is acting downward and there is a reaction force, R_3 , on the body from the adjacent wall.

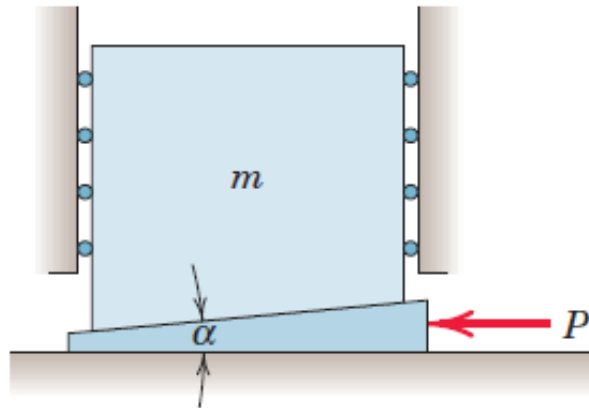


Figure 2.10: Wedge application

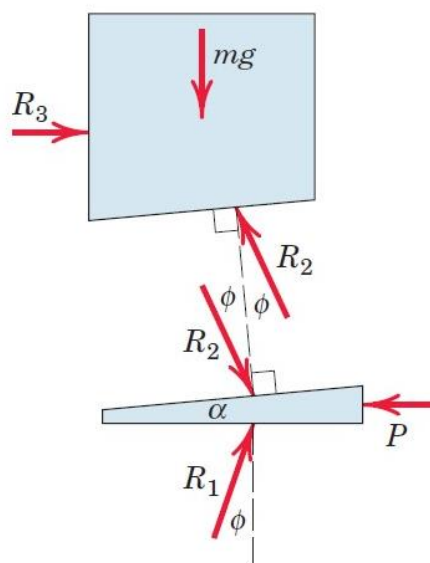


Figure 2.11: Free Body Diagram of wedge application

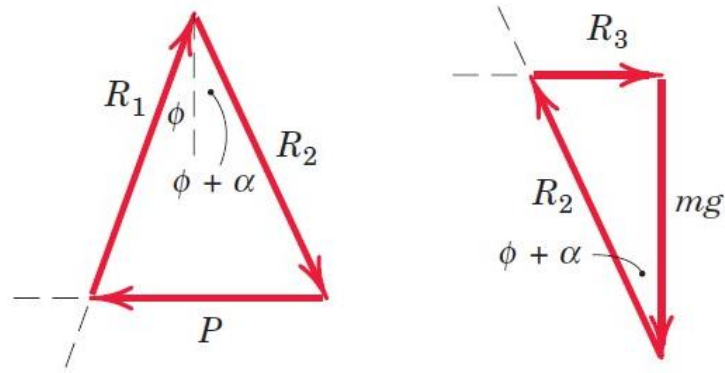


Figure 2.12: Geometrical representation of forces from wedge application

Finally from the free body diagram, a geometrical representation of the forces can be extracted as shown in Figure 2.12, where P is the force applied on the wedge from there R_2 can be calculated, and by using the second triangle R_3 will be calculated.

2.9 Strain gauge

In experimental stress analysis, it is not possible to measure stress but it can be calculated by using the measured strain and material's mechanical properties. Strain gauges is a sensor which measures the strain in term of change of resistance for electrical current in the wire while stretching or straining.

The working principle of the strain gauge is very simple as it consists of a metal wire which is shaped in a zigzagged pattern as shown in Figure 2.13 and the wire is mounted on a flexible plastic sheet [7]. Usually, the wire is of the circular cross-section. While straining the cross-sectional area of the wire is distorted and as the resistivity of a metallic material is inversely proportional to the cross-sectional area therefore, there is a definite change in the resistance of the wire.

In recent times, the wire-type strain gauge is replaced by the metal-foil strain gauges which work on the same principle but it is easier to cut a zigzag pattern on a sheet of metal than to make it from a wire which makes strain gauges more accurate.

The change of resistance in the strain gauge is determined by using the Wheatstone bridge which is discussed in detail in the next subsection.

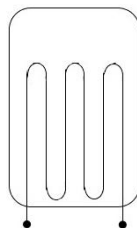


Figure 2.13: Pattern of strain gauge

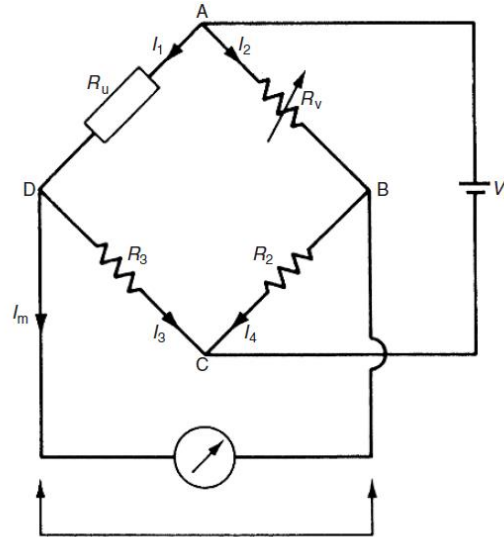


Figure 2.14: Wheatstone bridge

2.9.1 Wheatstone bridge

Wheatstone bridge is a Direct Current (DC) excited null-type bridge circuit. This was founded by Sir Charles Wheatstone, which is shown in Figure 2.14 [7]. Two resistors, R_2 and R_3 have equal and known resistances. R_v is the variable resistor and R_u is the unknown resistor.

Across the points A and C, a DC voltage is applied and the resistance of resistor R_v is varied until the voltage across the points B and D becomes zero. A highly sensitive galvanometer is used to measure this null point. From Equation (2-25), it can be seen that if both known resistances R_2 and R_3 are equal then it means R_u is equal to R_v . This method measures the unknown resistance accurately because variable resistance is derived from a resistance box.

$$R_u = \frac{R_3 R_v}{R_2} \quad (2 - 25)$$

Small changes in resistance can be easily measured by Wheatstone bridge therefore, it can be suitably used in strain gauges for measuring the change of resistance. There are three different configurations of this bridge circuit used in the measurement of strain as 1) Full bridge, 2) Half-bridge, and 3) Quarter bridge, as shown in Figure 2.15 [8].

In the experimental part of this thesis, a quarter bridge circuit with an external dummy strain gauge is used. Since the experiment is intended to be performed in ambient room temperature and for temperature compensation in the output usually, this method is used.

This method is most common for the measurement of strain on compression or tension bar. In this method, there is an active and a dummy strain gauge, as, by name, the active strain gauge measures the strain by applying it to the member which is under straining, and the dummy is attached to the member which is not under straining. An important condition for this method is to have the same material for both members, with dummy strain gauge as well as the member with an active strain gauge. The reason behind using this configuration is to compensate for the thermal effect on output as both dummy and active strain gauges are in the same temperature conditions.

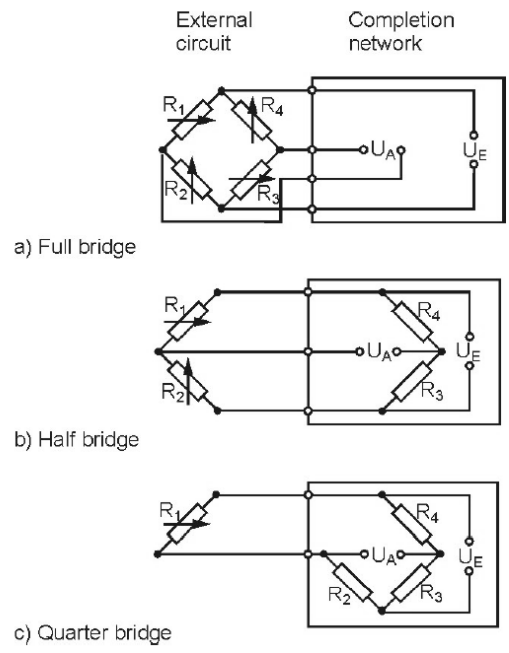


Figure 2.15: Three configurations of Wheatstone bridge for measuring strain

3 Theoretical Calculations

The main goal of this thesis is to compare the theoretical results of the Bondura bolt system with the experimental results as well as with results from the Finite Element Analysis. The other goal is to compare the bondura® pin system with the standard bolt for the same application.

Calculations for bondura® pin system are divided into three sections;

- Maximum possible preload in the central pin
- Effects on preload due to reduction of micro-asperities
- Wedge effect from the conical sleeves

For the standard bolts following are calculated;

- Preload as a function of torquing level and material strength
- Loss in preload as a function of reduction of micro-asperities.

3.1 Maximum preload in bondura® pin systems

In this section, maximum preload in central pins is calculated as a function of;

- Tightening screws strength
- Size and number of the tightening screws
- Tightening screw torquing level.

It is important to understand, two different sizes of bondura® pin systems are under study, the number of M10x35 and M10x60 tightening screws for both bondura® pin systems are shown in Table 3.1.

3.1.1 Maximum preload in the central pin as a function of Tightening screws strength

To make a comparison between screws of different strengths, a series of screws are used with the same geometrical properties but different mechanical strengths.

It is important to understand the nomenclature of the screw strength class. The number which is before the decimal point represents the 1/100th of breaking strength and the second term which is after the decimal, represents the yield strength of the screw in terms of percentage of breaking strength. For example, screw with a property class of 8.8 has a breaking strength of 800 MPa and a yield strength of 640 MPa.

Equation (2-3) is used to calculate the maximum shear stress. The maximum applied torque per

Table 3.1: Number of tightening screw in both bondura® pin systems

Tightening screw	Ø50 mm pin system	Ø80 mm pin system
M10x35	7	12
M10x60	7	6

M10 screw can be calculated by using the Equation (2-12). The radius c , for M10 screw, is equal to 5 mm and the polar moment of inertia, J , is calculated by using the following equation: $J = 0.5 \times \pi c^4$.

After calculating the maximum applied torque, the theoretical preload for a single M10 screw is calculated by using Equation (2-11) as shown in Table 3.2. The value of K is selected from Table 2.1, the bolt condition is lubricated and the diameter, d of M10 screw is 10 mm.

For Ø50 mm pin system, the preload per screw is multiplied with seven and for the Ø80 mm pin system multiply the preload per screw with twelve to calculate the theoretical value for maximum preload in both pin systems. The results for both pin systems are shown in Table 3.2.

3.1.2 Maximum preload in the central pin as a function of the size of tightening screws and different number of tightening screws

To analyze the effect of the different sizes of tightening screws, different screw sizes are selected ranging from M8 to M14 but with the same breaking strength of 1600 MPa.

Like the last section, maximum shear stress is 800 MPa which is calculated from the Equation (2-3). By using this value in Equation (2-12) for each screw, the value of maximum applicable torque is calculated. The Equation (2-11) is used to calculate the maximum preload per screw. Then, by multiplying this preload per screw with seven for the Ø50 mm pin system, and with twelve for the Ø80 mm pin system, the maximum preload for both pin systems are calculated. The maximum preload for different sizes of tightening screws for both pin systems are shown in Table 3.3.

Table 3.2: Preload per screw and maximum preload in both pin systems for different strength classes of tightening screws

Strength class of screws	Shear stress	Maximum applied torque	Preload per screw	Maximum preload in pin system	
				Ø50 mm	Ø80 mm
	MPa	Nmm	N	N	N
8.8	400	78539.82	43633.23	305432.62	523598.78
10.9	500	98174.77	54541.54	381790.77	654498.47
12.9	600	117809.72	65449.85	458148.93	785398.16
16.9	800	157079.63	87266.46	610865.24	1047197.55

Table 3.3: Preload per bolt and maximum preload in both pin systems for different sizes of tightening bolts

Tightening screw size	Maximum applied torque	Preload per screw	Maximum preload in pin system	
			Ø50 mm	Ø80 mm
	Nmm	N	N	N
M8	80424.77	44680.43	312763.00	536165.15
M10	157079.63	87266.46	610865.24	1047197.55
M12	271433.61	150796.45	1055575.13	1809557.37
M14	431026.51	239459.17	1676214.21	2873510.08

The number of tightening screws varies with the size of the load-bearing pin as in this thesis, the major focus is on two sizes of pins: Ø50 mm pin system has seven tightening screws on each side and Ø80 mm pin system has twelve tightening screws on each side. Therefore, to understand the effect of the different number of bolts, preload is calculated for a range of the number of bolts that have similar material and geometrical properties.

A similar process as in previous sections is used to calculate the preload per screw and maximum preload is calculated by multiplying the preload per screw with different numbers of tightening screws, as shown in Table 3.4.

3.1.3 Maximum preload in the central pin as a function of the torquing level of tightening screws

As discussed in Section 2.5, preload in bolted connection is only possible by the application of torque, and to achieve the desired preload it is important to understand the relationship between torquing level and preload. In this section, the maximum possible preload for both pin systems are calculated for different applied torques. Also in the experimental testing as well as in Finite Element Analysis, stresses and strains are measured for the range of applied torque, therefore, in this section average normal stresses and strains are also calculated for different levels of torque.

The M10 screw with a breaking strength of 1600 MPa is used. The maximum applicable torque, which is equal to 148.749 Nm is calculated by using the Equation (2-12).

Starting from zero, the torque level is increased by 20 Nm in every step. By selecting the experimental factor ‘K’ for lubricated bolt condition from Table 2.1, the Equation (2-11) is used to calculate the preload per screw. Then preload per screw is multiplied by seven for the Ø50 mm pin system, and by twelve for the Ø80 mm pin system to calculate total preload in both pins. The maximum preload at different levels of torque for both pin systems are shown in Table 3.5.

Equation (2-2) is used to calculate average normal stresses along the longitudinal axis for different levels of torque. Corresponding preloads from different levels of torque are used as applied force and it is assumed that the cross-section through the pin is constant. Average normal strains are calculated by using Equation (2-5) where the value of Young’s modulus is 210014.37 MPa. Both average normal stresses and strains for different levels of torque are shown in Table 3.6.

Table 3.4: Maximum preload for different number of tightening screw

Number of tightening screws	Maximum preload	Number of tightening screws	Maximum preload
	N		N
2	174532.93	12	1047197.55
5	436332.31	15	1308996.94
7	610865.24	18	1570796.33
9	785398.16	21	1832595.71

Table 3.5: Maximum preload for different levels of torque for both bondura® pin systems

Levels of torque	Preload per screw	Maximum preload in pin system	
		Ø50 mm	Ø80 mm
Nm	N	N	N
0	0	0	0
40	22222.22	155555.56	266666.67
60	33333.33	233333.33	400000.00
80	44444.44	311111.11	533333.33
100	55555.56	388888.89	666666.67
120	66666.67	466666.67	800000.00
140	77777.78	544444.44	933333.33
157.08	87266.11	610862.78	1047193.33

Table 3.6: Average normal stresses and strains for different levels of torque

Levels of torque	Ø50 mm bondura® pin system		Ø80 mm bondura® pin system	
	Average normal stress	Average normal strain	Average normal stress	Average normal strain
Nm	MPa	µm/m	MPa	µm/m
0	0	0	0	0
40	79.22	377.23	53.05	252.61
60	118.84	565.85	79.58	378.91
80	158.45	754.46	106.10	505.22
100	198.06	943.08	132.63	631.52
120	237.67	1131.69	159.15	757.83
140	277.28	1320.31	185.68	884.13
157.08	311.11	1481.37	208.33	991.99

3.2 Loss of preload due to the reduction of micro asperities

As discussed in Section 2.7, due to the plastic deformation of the micro asperities there is a reduction in preload over time. In this section, calculations for loss in preload are done with the assumption that the micro asperities are reduced one by third over the time.

Due to the geometrical challenges, it is not easy to calculate the elastic deformation of bolts by traditional methods therefore for this purpose, Boris recommends using Birger's recommendations. According to Birger's recommendations, compliance of bolt is calculated by using Equations (2-14) to (2-17) with the height of bolt head, 10 mm, length of the shank, 30 mm, and elastic modulus, 210014.37 MPa. With preload in M10 bolt equals 87266.46 N, Equation (2-18) is used to calculate elastic deformation of the bolt which is equal to 0.204 mm.

Similarly, to calculate the elastic elongation in flanges Equation (2-19) is used to calculate compliance of flanges with the diameter of the bolt head, 16 mm, the major diameter of the

bolt, 11 mm, and tangent of the cone of pressure angle, 0.5. And, Equation (2-20) is used to calculate the elastic deformation of flanges which is equal to 0.0463 mm.

There are three pairs of contacting surfaces and for the given material the mean height of micro asperities is approximately 5 μm . For the sake of understanding the effect of reduction of micro-asperities, it is assumed that over time micro-asperities are reduced by one-third of their height. With the assumed ratio of plastic deformation of micro asperities by the height, it is possible to calculate the decrease in elastic deformation by Equation (2-23) which is equal to 10 μm . By using Equation (2-22), the ratio of reduction of the initial elastic deformation is calculated as 0.0399.

Loss in preload for one M10 bolt is calculated by multiplying the ratio of reduction of the initial elastic deformation with the initial preload as in Equation (2-24) which is equal to 3483.9 N. There are seven M10 bolts in $\text{\O}50$ mm pin system and twelve in $\text{\O}80$ mm pin system. Loss in preload and remaining preload for $\text{\O}50$ mm and $\text{\O}80$ mm are presented in Table 3.7.

3.3 Wedge effect from the conical sleeves

In this section, the effect of wedging from the conical sleeve is calculated by using the method described in Section 2.9. A free-body diagram of a small section of the mating surfaces between the conical sleeve and coned nut is used for identifying the forces, as shown in Figure 3.1.

There is a load P from the applied torque of 70 Nm which is calculated using Equation (2-11), where the value of K is selected from Table 2.1, the bolt condition is lubricated. And the ‘ mg ’ is the weight force from the mass of the pin system. The inclination angle for the conical sleeve in both pin systems is equal to 12° .

Table 3.7: Loss in preload and remaining preload in both pin systems

Bondura® pin system	Loss in preload	Remaining preload
	N	N
$\text{\O}50$ mm	24387.26	586477.98
$\text{\O}80$ mm	41806.73	1005390.82

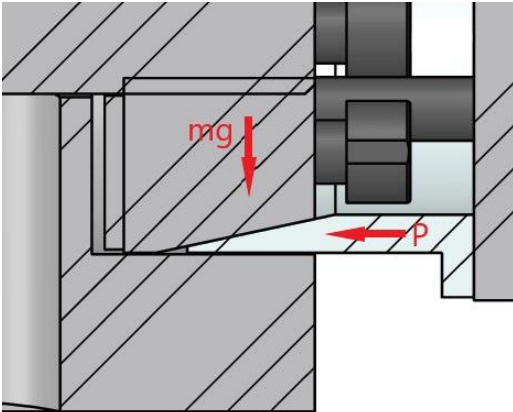


Figure 3.1: Section of the mating surfaces between conical sleeve and nut plate

As shown in Figure 3.2, there is a reaction force, R_3 , between the nut plate and jig's mating surface. R_2 is the force applied on both mating surfaces of nut and conical sleeve which is inclined to normal of the surface by the angle $\phi=30.96^\circ$ which, comes from the coefficient of friction. The coefficient of friction is approximately equal to 0.6 for dry steel on steel. There is also another reaction force, R_1 , between conical sleeve and jig which is also inclined by the same angle of $\phi=30.96^\circ$.

Mass on the wedge is calculated by using the following equation:

$$m = \frac{1}{2} m_{pin} + m_{shim} + m_{nut} + n_1 m_{b1} + m_{plate} + n_2 m_{b2}$$

where n_1 is the number of M10x35 bolts and m_{b1} is mass of M10x35 bolts and n_2 is number M10x60 bolts and m_{b2} is mass of M10x60 bolts on each side of bondura® pin system.

From the free body diagram, the graphical representation of the forces is extracted as shown in Figure 3.3. R_2 is calculated using the following equation:

$$R_2 = \frac{P}{\sin\theta}$$

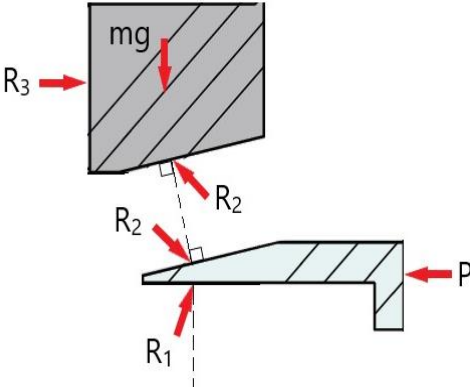


Figure 3.2: Graphical representation of the forces

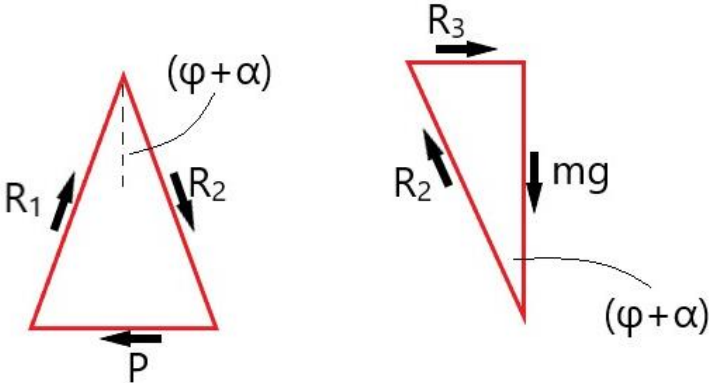


Figure 3.3: Reaction forces from wedge action of conical sleeve

where θ is the summation of α and φ .

Now, by using the other triangle R_3 is calculated by using the following equation:

$$R_3 = \sqrt{R_2^2 - mg^2}$$

There is already preload in the pin at this point so, stress is calculated by adding R_3 in that preload. All of the numerical results are presented in Table 3.8.

3.4 Standard bolts

To compare the standard bolts with bondura® pin systems two bolts are selected with the same diameter as the diameter of central pins. In this section, maximum possible preload is calculated for M50 and M80 standard bolts as well as the loss of preload due to a reduction in micro-asperities.

3.4.1 Maximum possible preload

To compare the maximum possible preload in standard bolt with the bondura® pin system, the maximum preload is computed in M50 and M80 bolts with a range of bolt property class.

The breaking strength is calculated as described in Section 3.1.1 then, Equation (2-3) is used to calculate the maximum shear stress. By using this shear stress value maximum applied torque for M50 and M80 bolts are calculated by using the Equation (2-12), as radius c , for M50 and M80 bolts are equal to 25 mm and 40 mm respectively and the polar moment of inertia J is calculated by using the following equation: $J = 0.5 \times \pi c^4$.

According to Boris, the value for experimental factor (K) is approximately equal to 2 for lubricated bolt condition, therefore, with Equation (2-11), maximum possible preload is calculated for both M50 and M80 bolts by using the calculated maximum applied torque. Preload is calculated for different bolt property classes are shown in Table 3.9 and Table 3.10 respectively for both bolts.

3.4.2 Loss of preload due to the plastic deformation of micro-asperities

The loss of preload in both bolts due to the plastic deformation of micro-asperities is calculated by the method described in Section 2.7. By using Briger's recommendations, compliance of bolt are calculated by using Equations (2-14) to (2-17) with the height of bolt head, 35 mm, length of the shank, 60 mm, and elastic modulus, 206 GPa for M50 bolt and height of bolt head, 51 mm, length of the shank, 60 mm, and elastic modulus, 206 GPa for M80 bolt. Equation (2-18) is used to calculate elastic deformations in both bolts.

Similarly, to calculate the elastic elongation in flanges Equation (2-19) is used for calculating compliance of flange with a diameter of the bolt head, 83 mm, the major diameter of the bolt, 53 mm for M50 bolt and with diameter of the bolt head, 115 mm, the major diameter of the bolt, 83 mm for M80 bolt.

Table 3.8: Numerical results of the wedge effect of conical sleeve for both pins

	Ø50 mm pin system	Ø80 mm pin system
Weight (mg)	36.27 N	63.27 N
Applied force (P)	35000 N	35000 N
R ₂	51378.87 N	51378.87 N
R ₃	51378.86 N	51378.83 N
Total load on central pin	662244.09 N	1098576.38 N
Stress in central pin	337.28 MPa	218.55 MPa

Table 3.9: Applied torque and maximum preload for different property classes of the M50 bolt

Property class of bolts	Shear stress	Maximum applied torque	Maximum preload
	MPa	Nmm	N
8.8	400	9817477.04	1090830.78
10.9	500	12271846.3	1363538.48
12.9	600	14726215.56	1636246.17
16.9	800	19634954.08	2181661.57

Table 3.10: Applied torque and maximum preload for different property classes of the M80 bolt

Property class of bolts	Shear stress	Maximum applied torque	Maximum preload
	MPa	Nmm	N
8.8	400	40212385.97	2792526.80
10.9	500	50265482.46	3490658.50
12.9	600	60318578.95	4188790.20
16.9	800	80424771.93	5585053.61

The tangent of the cone of pressure angle is 0.5 for both bolts. After that Equation (2-20) is used for calculating elastic deformations in the flanges.

There are four pairs of contacting surfaces and for the given material the mean height of micro asperities is approximately 5µm. For the sake of understanding the effect of reduction of micro-asperities, it is assumed that over the time micro-asperities are reduced by one-third of their height. With the assumed ratio of plastic deformation of micro asperities by the height it is possible to calculate the decrease in elastic deformation by Equation (2-23). Finally, with Equation (2-22), the ratio of reduction of the initial elastic deformation can be calculated.

Loss in preloads for M50 and M80 bolts are calculated by multiplying the ratio of reduction of the initial elastic deformation with the initial preload as in Equation (2-24) which are equal to 43114.3 N and 82027.7 N respectively.

3.5 Mating surface areas

One of the main ambitions behind the design of the bondura® pin system is to eliminate the radial and rotational movement of the fasteners in the flange joint. In standard bolts, the resistance between the mating surface of flanges and, bolt head and nut surface are responsible for avoiding radial and rotational movements as highlighted in Figure 3.4. Whereas, in the bondura® pin system the approximately the same amount of resistance is produced by the shims and surface of flanges. In addition to that, there are two conical sleeves to increase the surface area which ultimately increases the surface resistance.

Therefore to make a comparison between the approaches of both types of fasteners, mating surface area between flanges and the bondura® pin system and standard bolts are calculated in this section.

3.5.1 Mating surfaces area for standard bolts and flanges

As shown in Figure 3.4, the highlighted surface area between flanges and the bolt head and nut is calculated by using the following equation,

$$A = 2 \times \frac{\pi}{4} (d_1^2 - d^2)$$

where, d_1 is the diameter of bolt head and diameter of nut, and d is the diameter of the bolt. Numerical values for both M50 and M80 are presented in Table 3.11.

3.5.2 Mating surfaces area for bondura® pin systems and flanges

As mentioned before there are two surfaces in bondura® pin system for the purpose of

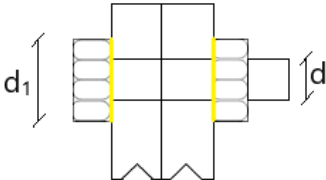


Figure 3.4: Highlighted mating surfaces between standard bolt and flanges

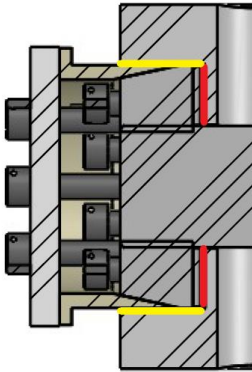


Figure 3.5: Highlighted mating surfaces between bondura® pin system and flanges

providing the surface resistance, one from the shims and the other from the conical sleeves as shown in Figure 3.5.

The mating area between conical sleeves and surface of flanges is calculated by using the following equation,

$$A_{CS} = 2\pi r h$$

where r is the radius of conical sleeve and h is the width of the conical sleeve.

Conical sleeves have four slots with the purpose of easy installation and the area of one slot is calculated as,

$$A_s = w \times r$$

where w is the width of the slot.

The mating area between shims and surface of flanges is calculated by using the following equation,

$$A_{sh} = 2 \times \frac{\pi}{4} (d_o^2 - d_i^2)$$

where d_o is the outer diameter of shim and d_i is the inner diameter of shim.

And finally, the total mating surface of the bondura® pin system and flanges is calculated by using the following equation,

$$A = 2 \times (A_{CS} - A_s + A_{sh})$$

Numerical values of both Ø50 mm and Ø80 mm pin systems are presented in Table 3.12.

Table 3.11: Mating surface areas between M50 and M80 bolt and surface of flanges

Standard bolt	Diameter of bolt	Diameter of bolt head	Diameter of nut	Mating surface area
	mm	mm	mm	mm ²
M50	50	83	83	6894.23
M80	80	115	115	10720.68

Table 3.12: Mating surface areas between Ø50 mm and Ø80 mm bondura® pin system and the surface of flanges

Bondura® pin system	Sleeve width	Sleeve radius	Area with slots	Outer diameter of shims	Inner diameter of shims	Area of shims	Total Mating area
	mm	mm	mm ²	mm	mm	mm ²	mm ²
Ø50 mm	23.24	50	14320.28	99	50.5	11389.45	256169.73
Ø80 mm	23.24	65	18610.92	129	80.5	15960.47	34571.39

4 Experimental work

One of the main tasks of this thesis is to evaluate the possible maximum preload from the bondura® pin system, which is calculated for different torquing levels in Section 3.1.3. To verify theoretical values an experiment is designed in which different levels of torque are applied on both pin systems. The purpose of the experimentation is to observe the stress in the central pin of the bondura® pin system so, instead of using a complete flange, a test jig, as shown in Figure 4.1, is used which is further bolted on the test tabletop to avoid any unwanted movements.

In experimental stress analysis, it is practically impossible to directly measure stress in a body and solution for that is to measure mechanical strain by using strain gauges, and then by using Young's modulus, the stress can be calculated.

Therefore, in this experiment normal stress along the axis of the central pin is measured by using two strain gauges which were connected parallel to each other at an angle of almost 180° on the pin, as shown in Figure 4.2.

4.1 Strain gauge

Many factors are involved in the selection of a strain gauge like material and geometry of the specimen, the nature of stress analysis, the environmental conditions of the testing place, and the available type of supporting equipment. In this experiment, normal stress along the axial axis is intended to measure a circular pin with the available hardware and software at the University of Stavanger. The central pin is made of ferritic steel and the experiment is intended to be done in an ambient room temperature environment. Therefore, based on these controlling factors, strain gauges of type KLY41 from HBM company were selected.

KLY41 is a Y series strain gauge with single measuring grid, this strain gauge is used for linear measurements of strain and it comes with 40 mm of Teflon coated connection wires as well as PVC-insulated ribbon cable [9]. According to the HBM website, Y strain gauges are universal strain gauges, whose measuring grid is made of constantan, which is an alloy of copper and Nickel, and the measuring grid carrier is made of polyimide. The reference temperature for this

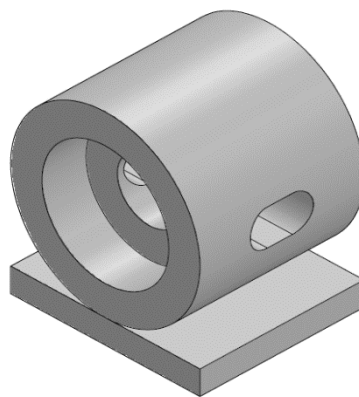


Figure 4.1: Test jig instead of complete flange

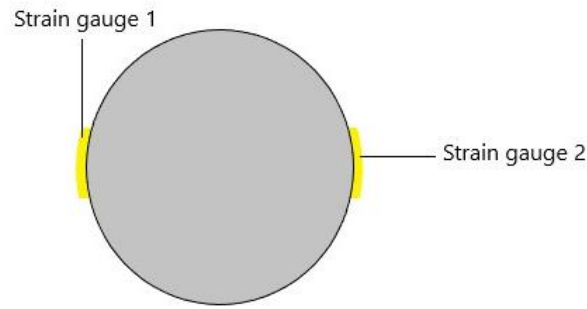


Figure 4.2: Locations of Strain gauges on central pin

strain gauge is 23°C and the operating range for static analysis is from -70°C to +200°C. The strain gauge which is selected for this experiment has 3 mm of grid length and 200Ω of grid resistance with a gauge factor of 2. A certificate from the HBM company is attached in Appendix B.

The method which is used in this experiment for the application of strain gauges is called the active dummy method. It is a widely used method for compensating thermally induced strains. In this method, two strain gauges are used and one of them is called active and the other is called the dummy strain gauge. The active strain gauge is bonded to the object which is intended to be under stress and the dummy strain gauge is applied on an object which is made of the same material as active but not under stress. It is very important that both objects are under the same temperature conditions because of which the thermally induced strains in both gauges will be equal and that is compensated in the output.

In this experiment, total four strain gauges are used on a single pin, two of those strain gauges are applied on the central pin with a difference of 180° as shown in Figure 4.3 for Ø50 mm pin system and two are applied as dummy strain gauges on a member which is made of the same material as a central pin as shown in Figure 4.4.



Strain gauge 1



Strain gauge 2

Figure 4.3: Active strain gauges on Ø50mm central pin

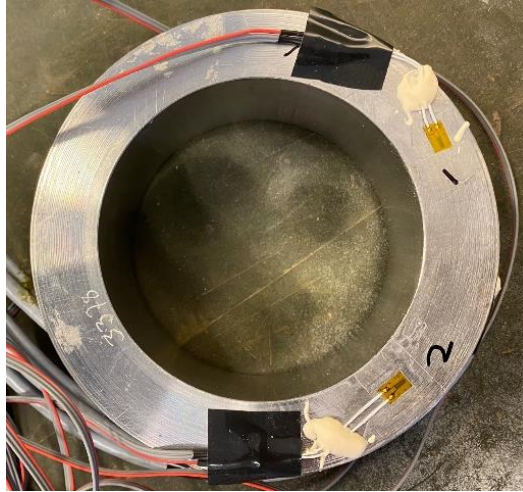


Figure 4.4: Dummy strain gauges

4.2 Data Acquisition System

The University of Stavanger has a Data Acquisition System or DAQ module from HBM company and it was one of the factors for selecting the strain gauges from the HBM company. This DAQ module consists of a measurement electronics known as Spider8 and software called Catman® professional.

Spider8 is a measurement electronics with multiple channels which is designed for dynamic and parallel measurement data acquisition using a computer. Spider8 is fully PC-controlled and does not need any further controls, other than just an ON/OFF switch. Installation and configuration are quite straight forward as the wires from both active and dummy strain gauges are soldered on a 15pin connector which can be easily connected to the Spider8. For the experimental stress analysis, the recommended version is the basic type of Spider8 with 600 Hz carrier frequency which is used in this experiment which is shown in Figure 4.5.

It is important to have compatible software for the hardware and recommendations from the manufacture of the hardware is always worth considering for this therefore, catman® professional from HBM company is used in this experiment. This software is multi-purpose software as it controls the settings for Spider8 as well as it provides digital display of data in



Figure 4.5: Basic type of Spider8 with 600 Hz

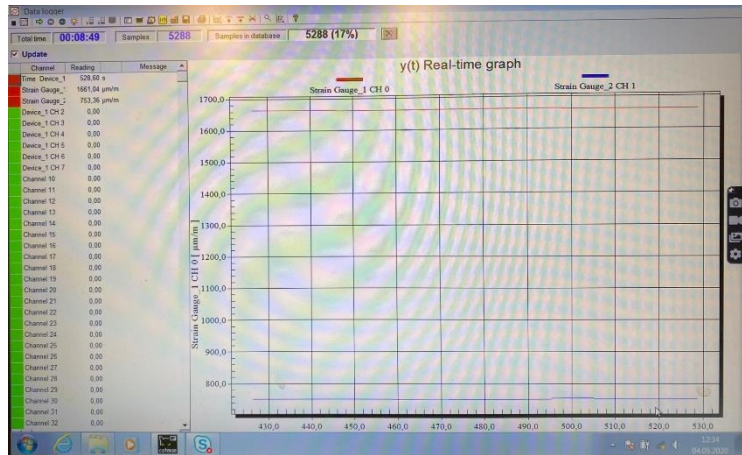


Figure 4.6: Real time data display for Ø50mm pin system

real-time as shown in Figure 4.6 for Ø50 mm pin system. This software also provides post-analysis functions as it has many options for data recording and data analysis.

4.3 Application of torque

For the application of controlled-load as discussed in Section 2.5.1, torque in this experiment is applied by hand using a torque wrench from USAG company [10], as shown in Figure 4.7. This torque wrench is based on the turn-of-the-nut method. This torque wrench has a range



Figure 4.8: Application of torque using USAG torque wrench



Figure 4.7: Dial of USAG torque wrench indicating range from 40 to 200 Nm

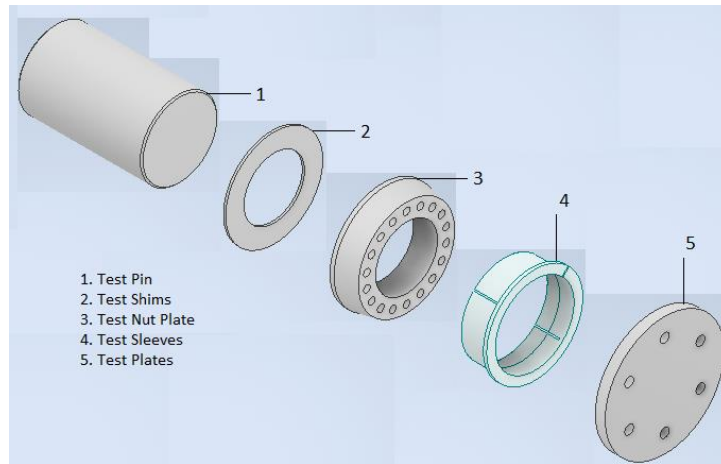


Figure 4.9: Sequence of different parts of bondura® pin systems

from 40 Nm to 200 Nm, the dial of the torque wrench is shown in Figure 4.8. This range is sufficient for this experiment as the maximum torque the bolt can have is 148 Nm. The certificate for the calibration for this torque wrench is attached in Appendix C.

4.4 Experiment

As it is mentioned above instead of using a complete flange, a test jig is used which is connected to the tabletop with 8 mm nut and bolt. Both M10x35 and M10x60 bolts are lubricated before the testing. Figure 4.9 is indicating the sequence of different parts of the bondura® pin system and according to that the central pin, which has two strain gauges bounded on it, is inserted in the test jig and then both shims go on each side of the pin.

Coned nuts are screwed on both sides of the pin which are also lubricated for easy installation. By using the recommended cross-pattern from ASME PCC-1-2010 [11], M10x35 tightening screws are screwed on both sides simultaneously with torque wrench starting from 40 Nm, as it is the minimum limit of the available torque wrench, and after that torque is increased by 20 Nm in every step until the screw breaks which is shown in Figure 4.10 for both Ø50 mm bondura® pin system and Ø80 mm bondura® pin system.

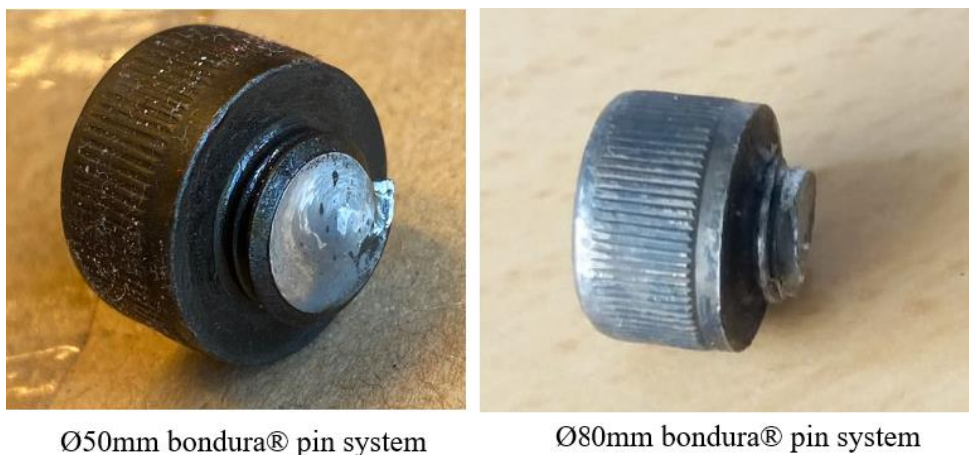


Figure 4.10: Broken M10x35 tightening screws for both bondura® pin systems

For measuring the effect of conical sleeves on the preload, insert the conical sleeves are inserted on both sides. The plates are attached on both sides by screwing the M10x60 bolts. With a torque wrench, the 70 Nm torque is applied by using the recommended cross-pattern from ASME PCC-1-2010.

Measured strains from both strain gauges are shown in Table 4.1 and measured stresses are shown in Table 4.2 for both Ø50 mm bondura® pin system and Ø80 mm bondura® pin system for a range of applied torque. As discussed in Section 3.3, the strain is increased in the central pin by inserting the conical sleeves as shown in Table 4.3.

Table 4.1: Measured strains due to applied torque for both pin systems

Applied torque	Measured Strain					
	Ø50 mm bondura® pin system			Ø80 mm bondura® pin system		
	SG-1	SG-2	Average	SG-1	SG-2	Average
Nm	µm/m	µm/m	µm/m	µm/m	µm/m	µm/m
0	0	0	0	0	0	0
40	368.4	168.4	268.4	230	213	221.5
60	608.8	294.2	451.5	320	303	311.5
80	873.12	378.2	625.66	438	394	416
100	1104.0	479.0	791.5	614	556	585
120	1356.0	583.2	969.6	684	668	676
140	1535.7	668.7	1102.2	790	789	789.5
160	■	■		■	■	

Table 4.2: Stresses from measured strains for both pin systems

Applied torque	Measured Stress					
	Ø50 mm bondura® pin system			Ø80 mm bondura® pin system		
	SG-1	SG-2	Average	SG-1	SG-2	Average
Nm	MPa	MPa	MPa	MPa	MPa	MPa
0	0	0	0	0	0	0
40	77.37	35.37	56.37	48.30	44.73	46.52
60	127.86	61.79	94.82	67.20	63.63	65.42
80	183.37	79.43	131.40	91.99	82.75	87.37
100	231.86	100.60	166.23	128.95	116.77	122.86
120	284.78	122.48	203.63	143.65	140.29	141.97
140	322.52	140.44	231.48	165.91	165.70	165.81
160	■	■		■	■	

Table 4.3: Effect of conical sleeves in terms of measured strains

Bondura® pin system	Applied torque	Measured Strain		
		SG-1	SG-2	Average
	Nm	µm/m	µm/m	µm/m
Ø50 mm	70	1622.0	751.32	1206.66
Ø80 mm	70	915	818	866.5

5 Finite Element Analysis

In the modern era of technology fast and efficient computer machines are working as a driving force, helping in every field to make tasks easier and cost-efficient. Engineers and scientists are working continuously for many decades for developing tools for Finite Element Analysis or FEA and now many tools are available in the market which can effectively predict the physical behavior of complicated problems.

The original purpose of developing the Finite Element Analysis was to solve the complex solid mechanics problems numerically. FEA has been proven a much-needed tool for designers as it reduces the number of prototypes and design time as well as it provides the opportunity to optimize by varying the design parameters.

In modern industries, precise use of resources is very critical which sometimes leaves limited finances for research and development, and performing an experiment is an expensive adventure and, in such situations, using Finite Element Analysis is inevitable.

Even though licensees for professional versions of some modern software are quite expensive but for the academic researcher, these software companies provide free academic versions for a certain period. This helps these companies in the further development of their software and at the same time provides academic researchers a great opportunity to explore these products.

In Finite Element Analysis generally, geometry is developed according to the design requirement on Computer-Aided Drawing or CAD software like Creo, Inventor, Solid works, etc. And the simulations and post-processes are done on different software which is specially designed for different design procedures like ABAQUS, LS-DYNA, RADIOSS, ANSYS, etc. Even though new versions of some software can perform both tasks, but their capabilities are limited.

In this thesis, one of the major tasks is to find out the preload of the bondura® pin system which is provided by the M10x35 bolts and to perform the stress analysis on the central pin. An experiment was performed to examine the stresses in the pin and now in this part of the thesis, stress analysis of the central pin is performed to find out the stress distribution in the central pin.

In this thesis, the CAD model was developed on the academic version of Autodesk Inventor, and Finite Element Analysis was done on the workbench of ANSYS software which is one of the best known FEA tools for 2D and 3D problems.

Drawings for both pins were provided by the Bondura Technology AS, which were slightly changed in Autodesk Inventor, based on the same assumption which was undertaken in the theoretical section for the analysis. Drawings from Bondura Technology AS are available in Appendix D.

5.1 Preparation for Analysis

For simulations in ANSYS Workbench, some of the pre-processes must be done as Selecting or adding material, setting up the coordinate system, generating a suitable mesh, applying constraints, and applying the loads. If a simulation is being done on an assembly then it is also important to define the relationship between mating parts but in this analysis, simulation is being done on a single part. In the following subsection, these steps are discussed briefly for the bondura® pin.

5.1.1 Material

In the pre-process section, ANSYS Workbench has an option of Engineering Data which provides the opportunity to select a material from the library of Workbench or material can be added to the library. To make analysis synonymous with the theoretical work the bondura® pin's material was added in the library as shown in Figure 5.1. Material properties of different parts of bondura® bolt systems are added in Appendix A.

5.1.2 Coordinate System

Defining an accurate coordinate system in simulation tools is one of the most important tasks to avoid errors in the results. In ANSYS workbench, it is possible to either choose the global coordinate system or have a local coordinate system. There are three predefined global coordinate systems in the ANSYS software: Cylindrical, Cartesian, and spherical.

For bondura® central pin, the focus is to find the normal stress along the longitudinal axis so, from the global coordinate system, the x-axis was selected as the longitudinal axis, as shown in Figure 5.2 for 50 mm central pin.

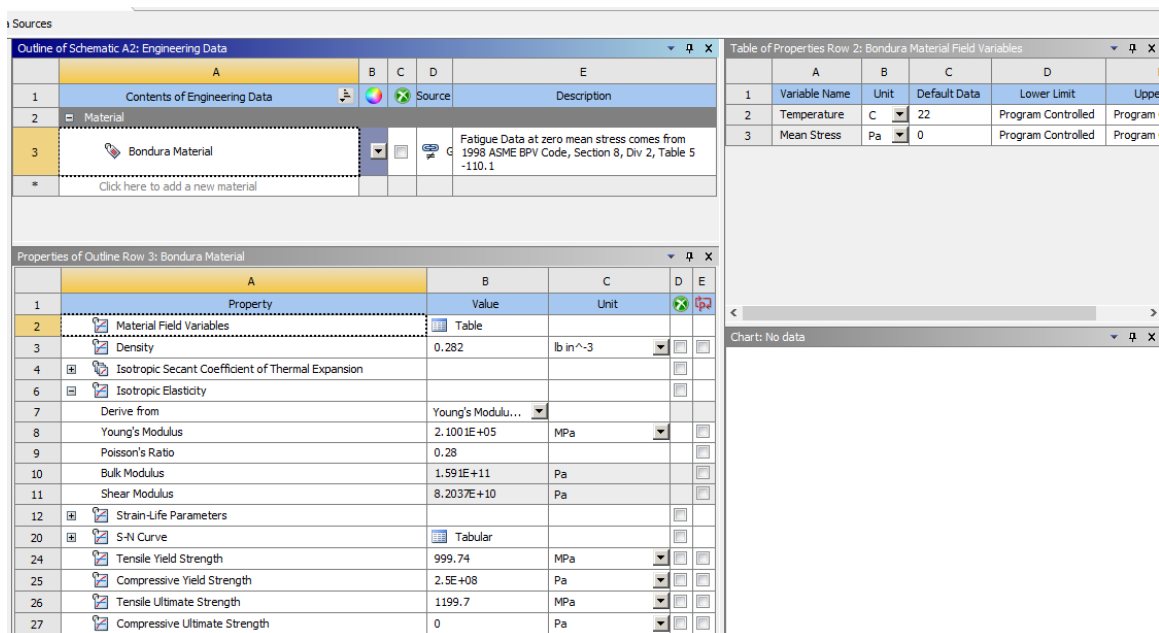


Figure 5.1: Bondura® material in the library

5.1.3 Meshing

In Finite Element Analysis accuracy, processing time, and convergence of the solution is defined by the meshing. For complex geometries, ANSYS workbench provides different controlling factors to define suitable meshing. In this analysis, simulations are done on the central pin which has a constant cross-section throughout its length therefore meshing was defined by sizing a single element for both pins, as shown in Figure 5.3 for 50 mm central pin. It is important to mention here that, in the academic version of ANSYS defining the size of the element is very limited and meshing was done on both pins with the smallest possible size of the element.

5.1.4 Constraints and loads

In ANSYS workbench a variety of options are available for application of constraints and loads depending on the design requirement. For stress analysis in the longitudinal axis of the central pin, on one circular face *Fixed Support* was applied as shown in Figure 5.4 for 50 mm central pin. And on the other circular face of pin normal force in newton was applied, as shown in Figure 5.5 for 50 mm central pin.

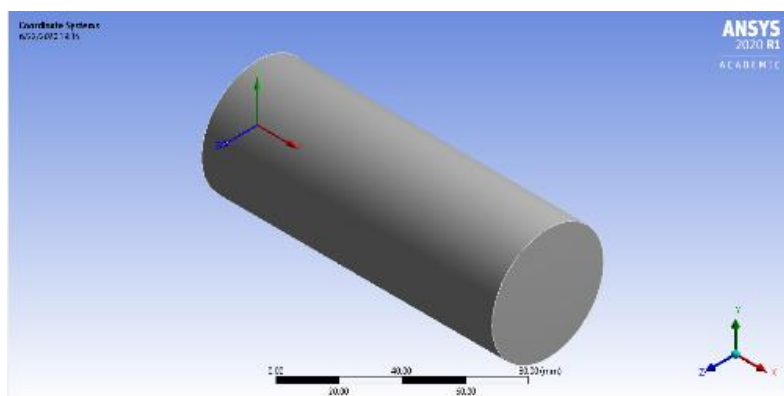


Figure 5.2: Coordinate system for 50mm central pin

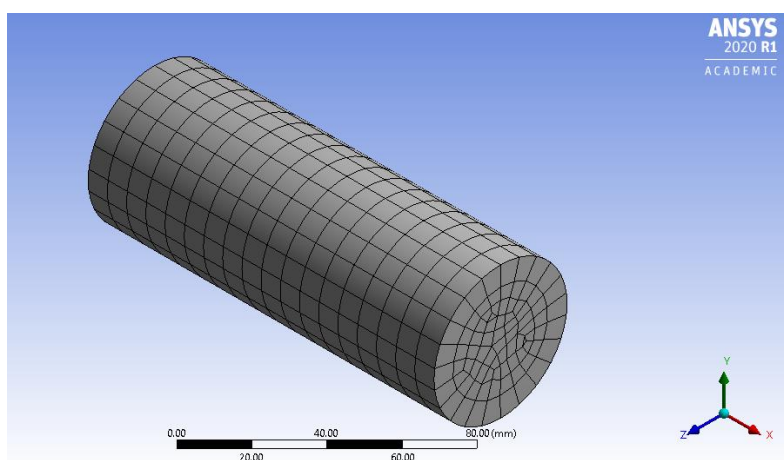


Figure 5.3: Meshed view of 50mm central pin

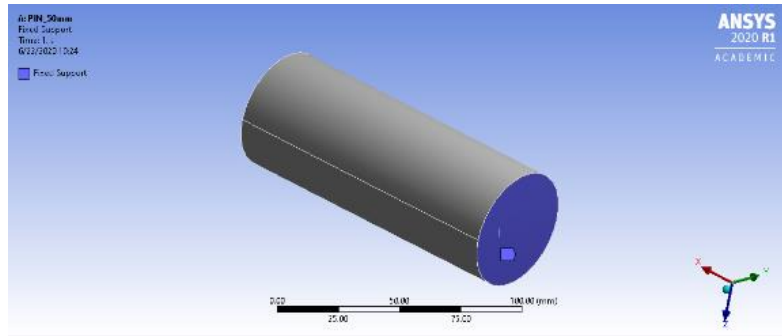


Figure 5.4: Fixed support on 50mm central pin

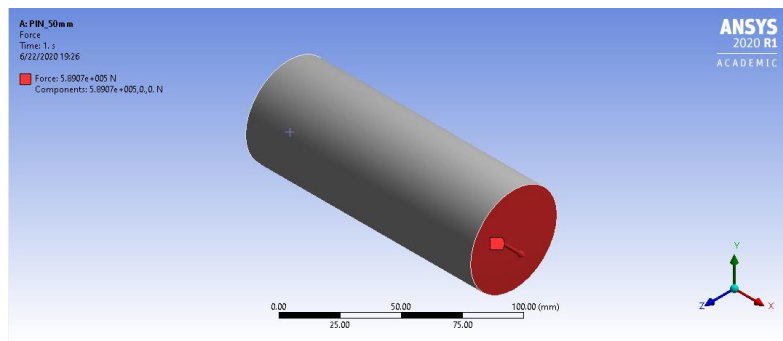


Figure 5.5: Load applied on the 50mm central pin

5.2 Solution

It is possible to have a variety of outputs for stress, strain, and displacement in static structural analysis. As discussed above the desired output from FEA is the distribution of longitudinal stress therefore, normal stress along x-axis was selected for output, as shown in Figure 5.6 for 50 mm central pin. After all these the program was commanded to run.

The applied load is increased in every step until the maximum calculated preload and the relative average normal stress was recorded which are shown in Table 5.1 for 50 mm central pin and in Table 5.2 for 80 mm central pin.

Table 5.1: Average normal stress and strain for applied torque and preload in 50 mm central pin

Applied torque	Average normal stress	Average normal strain	Preload
Nm	MPa	$\mu\text{m/m}$	N
0	0	0	0
40	79.25	372.30	155555.56
60	118.88	558.50	233333.33
80	158.51	744.68	311111.11
100	198.13	930.85	388888.89
120	237.76	1117.00	466666.67
140	277.38	1303.20	544444.44
157.079	311.22	1462.20	610862.78

Table 5.2: Average normal stress and strain for applied torque and preload in 80 mm central pin

Applied torque	Average normal stress	Average normal strain	Preload
Nm	MPa	$\mu\text{m/m}$	N
0	0	0	0
40	53.41	247.87	266666.67
60	79.667	371.8	400000.00
80	106.22	495.73	533333.33
100	132.78	619.67	666666.67
120	159.33	743.6	800000.00
140	185.89	867.53	933333.33
157.079	208.57	973.36	1047193.33

From Figure 5.6 it can be observed that the maximum area of the pin is under a low level of stress and just towards the edges, it is slightly in the upper level of stress. The rest of the screenshots for the normal stress along the x-axis are attached in Appendix E and Appendix F for $\varnothing 50$ mm pin system and $\varnothing 80$ mm pin system, respectively.

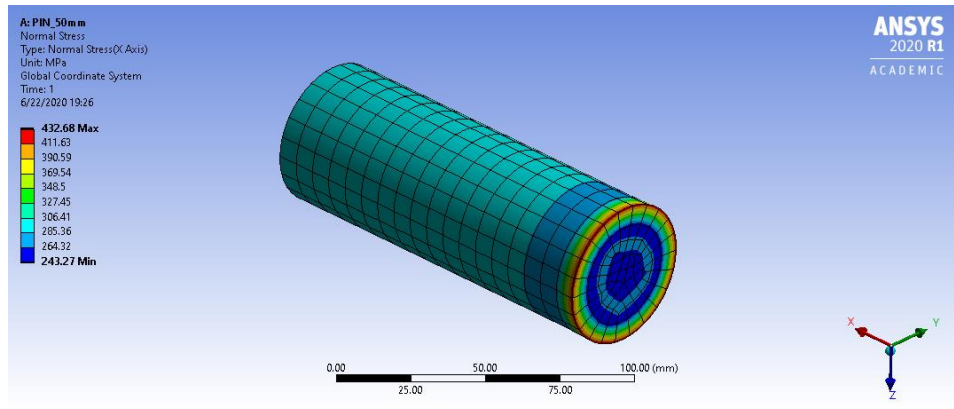


Figure 5.6: Normal stress along x-axis for 50mm central pin

6 Discussion

In the previous three chapters theoretical, experimental, and finite element analysis for bondura® pin systems are done, as well as the necessary calculations for standard bolts to make a comparison. This chapter contains the discussions on the findings from all those analysis and comparison with the standard bolts. Also, at the end some justifications for the errors in the experimental analysis.

This chapter starts with the discussion of different factors involves in the determination of maximum possible preload from the bondura® pin systems like strength, size, and the number of the tightening screws. Next to that, preload in the bondura® pin system for different levels of torque is discussed with the help of theoretical, experimental, and finite element analysis. Also, there is a discussion about the wedge effect from the conical sleeves.

After that, there is a comparison of bondura® pin systems with standard bolts in terms of preload capability, loss in preload due to plastic deformation of micro-asperities, and mating surface area. In the end along with the justification of errors in the experimental analysis, there are some points regarding the different possibilities for the bondura® pin systems based on the work carried out for this thesis.

6.1 Maximum possible preload

Preload in the bondura® pin system comes from the torque applied to the M10x35 mm tightening screws. Three major factors can limit the maximum possible preload and those are strength, size, and number of tightening screws. In Section 3.1, several calculations are done to understand the effects of changing these factors.

In the Sub-section 3.1.1, maximum possible preload in Ø50 mm and Ø80 mm bondura® pin system for different strength classes of M10X35 tightening screws are calculated and are presented in Table 3.2. Figure 6.1 is showing a graph based on that data, which is indicating that with the increment in the strength of tightening screw, preload in the central pin is also increasing linearly. This is because at higher strengths the M10X35 screw can bear higher torque which means higher preload per screw. But in Ø80 mm pin system preload in the central pin is higher because it has twelve M10x35 tightening screws as compared to seven in Ø50 mm pin system. The maximum preload is possible from the tightening screws of 16.9 strength class which are being used in the current design of the bondura® pin system.

Size of tightening screws in both bondura® pin systems is the same as M10 but to analyze the effect of different sizes of tightening screws, maximum preload is calculated in Sub-section 3.1.2 for different sizes of screws. A graphical representation of the data from Table 3.3 is shown in Figure 6.2, which is indicating that preload capability is increasing with the size of the tightening screw, and before M14 screw the increment is above the straight line. This trend can be helpful while considering the possible ways to improve the preload capability of the bondura® pin system.

Even though increasing the number of M10 tightening screws means the increment in the size of the coned nut and ultimately the whole pin system but just to have an idea about the effect of increasing the number of tightening screws, maximum possible preload is calculated for a series of the number of screws in Section 3.1.2. By using the data available in Table 3.4 a graphical aid is presented in Figure 6.3, which is indicating that with the increment in the number of tightening screws maximum preload in the central pin is also increasing in the straight line.

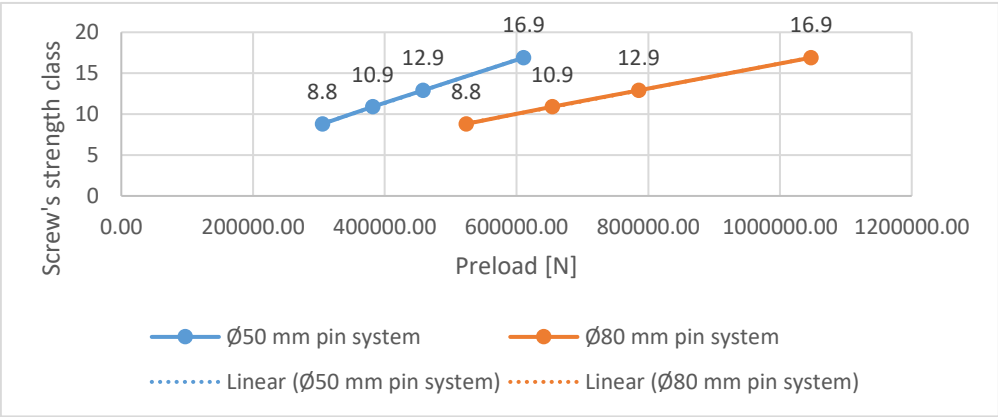


Figure 6.1: Relationship between strength of M10x35 tightening bolts and preload in pin

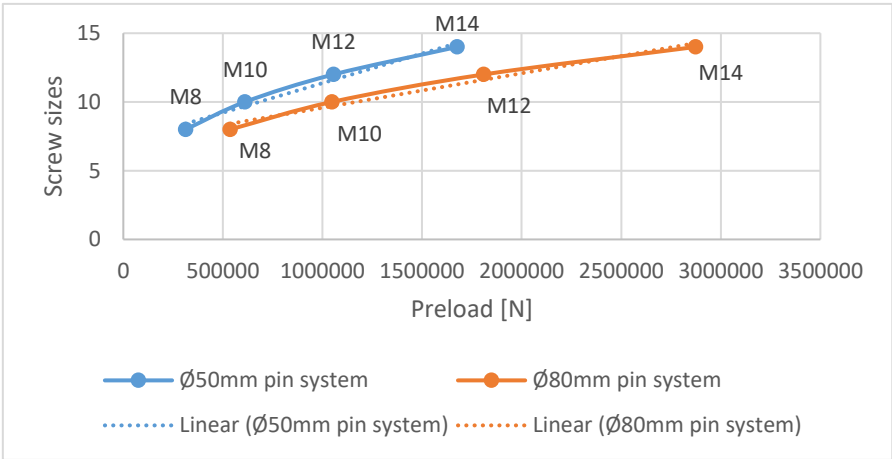


Figure 6.2: Relationship between screw sizes of 16.9 strength class and preload

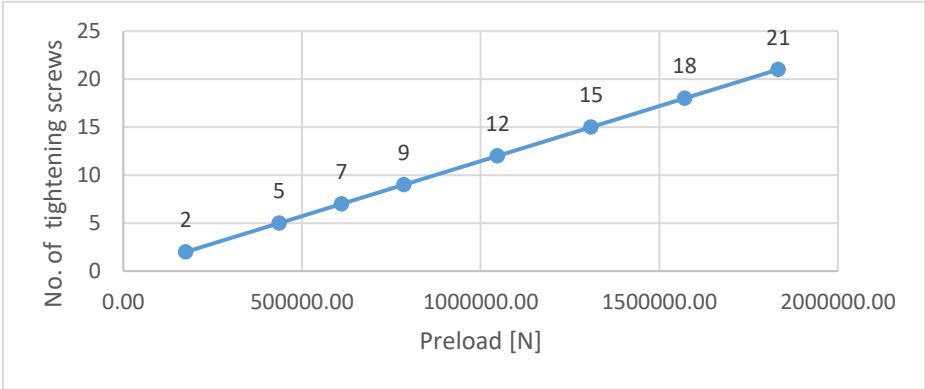


Figure 6.3: Relationship between number of tightening screws and preload

6.2 Torquing level of tightening screws

One of the major tasks of this thesis was to analyze the preload in the central pin for different levels of torque. For this purpose, preload in the central pin for different levels of torque is calculated in Sub-section 3.1.3. To verify the calculated results an experiment is designed in Chapter 4 to measure the strain in central pin and those values of strain are used to calculate the normal stress along the longitudinal axis and preload in the central pin, as shown in table 6.1. Also, in Chapter 5 simulations on ANSYS are done to measure the average normal stress and to visualize the stress distribution in the central pin for different levels of applied torque.

As shown in Figure 6.4 which is based on Table 3.4, the maximum possible preload is increasing in a straight line for both bondura® pin systems with the increment in the level of torque. The same trend can be observed from Figure 6.5 which is based on the results from the experiment.

In the finite element analysis, the average normal stress along the longitudinal axis is measured for different levels of preload from the applied torque which is presented in Table 5.1 and Table 5.2 for Ø50 mm and Ø80 mm bondura® pin system, respectively. Based on that data, a graph is presented in Figure 6.6 which is also indicating the same trend that the stress along the longitudinal axis is increasing with the increment of torque.

The purpose of simulating the central pin at different levels of torque in the ANSYS is to visualize the distribution of stress. Figure 6.6 and Figure 6.7 are showing the stress distribution at the maximum possible applied torque, 157.08 Nm, for Ø50 mm and Ø80 mm bondura® pin system, respectively. From these presentations, it can be observed that even at the maximum possible torque level of M10x35 tightening screws the stress in the maximum area of the pins is at the low level. This means the central pin is much more capable of containing the stress before going to plastic deformation. In Sub-section 4 of this chapter, there is a discussion on some possibilities to increase the preload capability of the bondura® pin system.

Table 6.1: Stress and preload for both bondura® pin systems calculated from measured strain

Applied torque	Measured stress		Measured preload	
	Ø50 mm pin system	Ø80 mm pin system	Ø50 mm pin system	Ø80 mm pin system
Nm	MPa	MPa	N	N
0	0.00	0.00	0.00	0.00
40	77.37	48.30	151914.25	242798.89
60	127.86	67.20	251046.14	337807.16
80	183.37	91.99	360041.73	462373.55
100	231.86	128.95	455247.93	648167.48
120	286.88	143.65	563286.84	722062.80
140	322.94	165.91	634089.43	833961.42

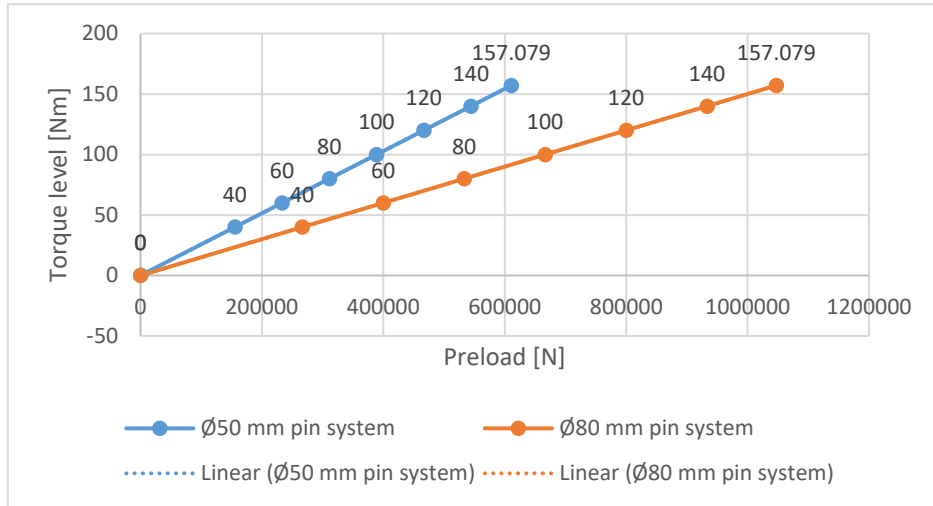


Figure 6.4: Relationship between torque level and calculated preload for M10x35-16.9 tightening screws

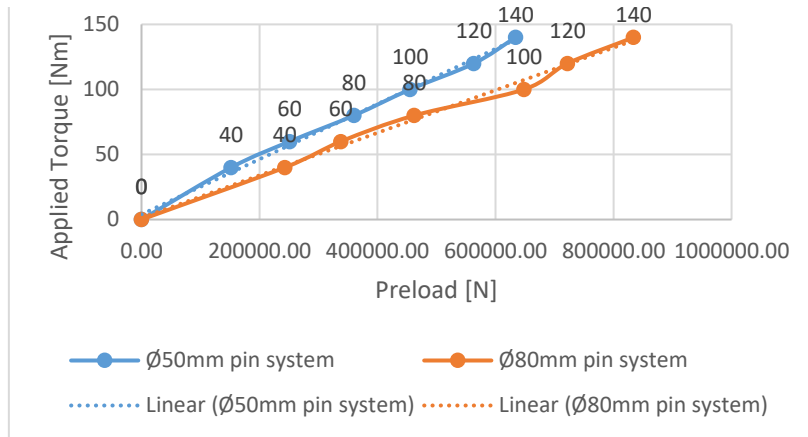


Figure 6.5: Relationship between applied torque level and measured preload from experiment for both pin systems

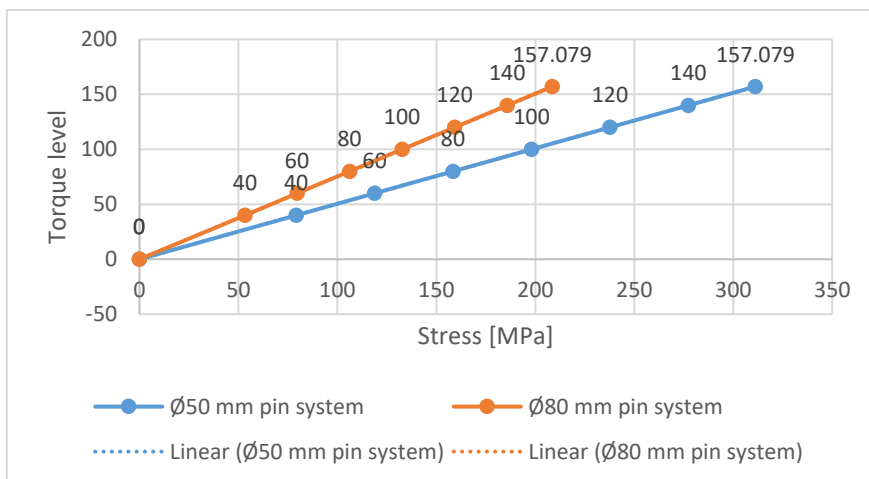


Figure 6.6: Relationship between torque level and average normal stress from finite element analysis for both pin systems

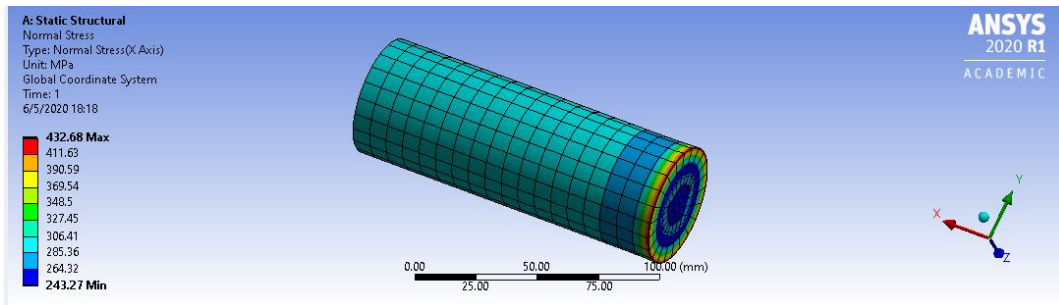


Figure 6.7: Stress distribution at 157.08 Nm torque in Ø50 mm pin system

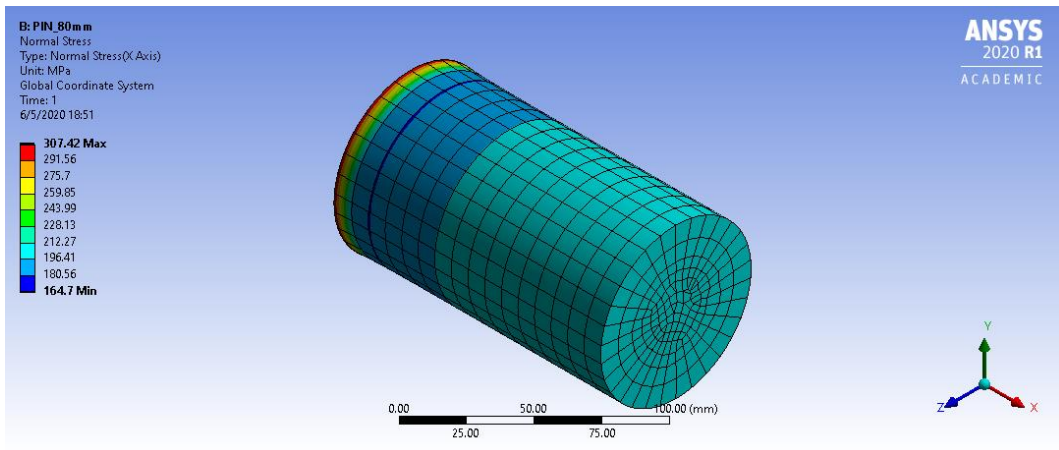


Figure 6.8: Stress distribution at 157.08 Nm torque in Ø80 mm pin system

6.3 Wedge effect from conical sleeves

The bondura® pin system is designed with the intention of not having any effect from the M10x60 tightening screws which does not affect directly but, they push the conical sleeve and it is possible to have a wedge effect from these sleeves. Calculations are performed in Section 3.3, which shows a member of the reaction force due to the wedge effect add the preload in the central pin. The applied torque is 70 Nm but the difference for Ø50 mm pin system is higher because of the smaller cross-sectional area compare to Ø80 mm pin system.

To verify this addition of preload, in the experimental work strains are measured after applying torque on the M10x60 tightening screws for both bondura® pin systems, which also shows the increase in the normal stress for both pin systems. Table 6.2 presents the calculated and experimental values of previous stress from M10x35 tightening screws, new stress after the application of torque on the M10x60 tightening screws, and the amount of stress increased due to wedge effect of conical sleeves. Even though the difference between the calculated and experimental value is high for both pin system but this does verify the increment of preload in central pin due to the wedge effect of conical sleeves.

As shown in Figure 3.2, there is a reaction force R_3 which is being applied on the coned nut and it poses a threat of making the pin system lose preload if R_3 becomes very high but to make a final comment on this further analysis is required which is not in the scope of this thesis.

Table 6.2: Stress in central pin due to the wedge effect from calculations and experiment

Bondura® pin systems	Previous stress in central pin		New stress in central pin		Stress added due to the wedge effect	
	Calculated	Experimental	Calculated	Experimental	Calculated	Experimental
	N	N	N	N	N	N
Ø50 mm	311.11	322.94	337.28	340.64	26.17	17.70
Ø80 mm	208.33	165.91	218.55	192.16	10.22	26.25

6.4 Comparison with standard bolts

In this section, the bondura® pin system is compared with standard bolt on three different factors,

- preload capability
- loss in preload due to plastic deformation of micro-asperities
- mating surface area.

For the sake of comparing the preload capability of bondura® pin system with the standard nut and bolt, maximum preload is calculated for two, M50 and M80 bolts are calculated in Section 3.4. Table 6.3 is presenting the maximum possible preload for both bondura® pin systems and standard bolts with a strength class of 8.8, along with the differences in preloads. The preload from the standard bolts are higher than the preloads from the bondura® pin systems.

To understand further the capability of maximum preload from bondura® pin systems and standard bolts a comparison has created with an assumed flange connection. Table 6.4 is showing the number of fasteners required to use for having a connection where the desired preload in flange connection is equal to 11170107.2 N. The required number of fasteners is relatively quite high for bondura® pin system.

According to Boris, the plastic deformation of micro-asperities in small bolts is significantly higher for low property class bolts as, elastic deformation while tightening is short for smaller bolts. As shown in Table 6.5, percentage loss in the initial preload is slightly higher in both bondura® pin systems as compared to standard bolts and in standard bolt loss in preload for M50 is higher than M80.

Loss in preload for both bondura® pin systems is the same because both have the same M10 bolt as the tightening bolt but the number of M10 bolts is different for both systems. There is an interesting point that regardless of the number of M10 bolts, loss in preload is the same for both pin systems.

One of the main reasons for the design of the bondura® pin system is to eliminate the possibility of radial movements in flange joints and the element of the pin which is intended to achieve that is the conical sleeve. As the conical sleeve is there to increase the surface resistance between mating surfaces of the bondura® pin system and the flange.

By using this conical sleeve, mating surfaces area between the fastener and the flange increases quite incredibly as shown in Table 6.6, the difference between the mating surface area for M50 and Ø50 mm bondura® pin system is 18725.51 mm² and for M80 and Ø80 mm bondura® pin system is 334749.94 mm².

Other than the increment in the mating surface areas, as shown in Figure 6.9 there is a component of reaction force R_2 from the wedge effect of the conical sleeve, which is calculated in Section 3.3. This component of reaction force is applying load on the conical sleeve towards the flange surface which also keeps the bondura® pin system from moving radially.

Considering both factors it is safe to say that the bondura® pin system is fully capable of avoiding any radial or rotational movements in the flange joint.

Table 6.3: Difference between preloads of bondura® pin systems and standard bolts

	50 mm	80 mm
Bondura® pin system	610862.78 N	1047197.55 N
Standard bolts	1090830.79 N	2792526.8 N
Difference	-479968.01 N	-1745329.25 N

Table 6.4: Required number of fasteners for the desired preload

Type of fastener	Required number of fastener(s)
Ø50 mm bondura® pin system	19
Ø80 mm bondura® pin system	11
M50	10
M80	4

Table 6.5: Loss in preload for bondura® pin systems and standard bolts

Fastener	Loss in Preload N	Initial maximum preload N	Loss from initial preload %
Ø50 mm pin system	24387.26	610865.24	3.99
Ø80 mm pin system	41806.73	1047197.55	3.99
M50	43114.35	1090830.78	3.95
M80	82027.69	2792526.8	2.94

Table 6.6: Mating surface area for different types of fasteners

Fastener	Mating surface area (mm ²)
M50	6894.22
M80	10720.68
Ø50 mm bondura® pin system	25619.73
Ø80 mm bondura® pin system	345470.62

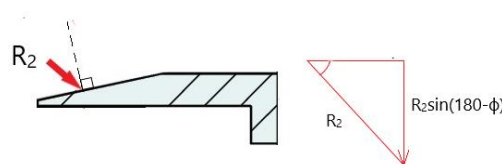


Figure 6.9: Component of reaction force R_2 from wedge effect of conical sleeve

6.5 Possibilities for bondura® pin system

From the previous three sections, it is concluded that standard bolts provide more preload and bondura® pin systems provide more safe design regarding the radial and rotational movements. Therefore, to have the best solution it is important to increase the maximum preload capability of bondura® pin system or to use both bondura® pin system as well as standard bolts in an optimized manner.

To have an optimized solution for a problem several factors need to be considered such as the nature of applied load as well as the size of flanges because the overall diameter of bondura® pin systems needs bigger space comparative to standard bolts. A mathematical model can be created to design a perfect solution for any problem using both bondura® pin system and standard bolts.

One of the main concerns regarding the bondura® pin system is the capability to produce preload as it is comparatively lower than the standard bolts. The preload in bondura® pin systems comes from the torque applied to the M10x35 tightening screws and to increase preload if applied torque is increased that will break M10 bolt as happened in the experiment which means it is not possible to increase the preload by just increasing the torque level. That solution must come either from the size factor or the number of tightening screws.

As discussed earlier, with the increment in the number of bolts preload capability will also be increased in straight line, as Ø80 mm pin system has more tightening screws and it has the capability of producing higher preload compare to Ø50 mm pin system. Therefore, it is important to look for the possibilities to increase the number of tightening screws.

The central pin behaves like a beam under tension loading which means only one side of loading is effective for producing preload as the other side of loading is there just to have an opposite direction loading. To reduce the cost of bondura® pin systems one side of assembly can be replaced by a simple standard nut and the size of coned nut can be increased to have space for more M10 bolts.

One other factor to gain more space for M10x35 bolt in the nut plate is to reduce the number of M10x60 bolts as the only purpose of these bolts is to maintain the continuous load throughout the conical sleeve which can be achieved with the lower number of M10x60 bolts as in Ø80 mm pin system.

The one other way to increase the number of tightening screws with the same geometric properties of the pin system is to reduce the size of screws responsible for producing the preload. To analyze the effect of reducing the size of tightening screws to M8 let us calculate the maximum possible preload.

With a fixed central pin size e.g. Ø80 mm pin system, there are twelve M10 tightening screws on each side with the 1.45 mm clearance between two bolts. By keeping the same clearance and the available circumference of 314.16 mm, it is possible to have sixteen M8x35 mm tightening screws. The preload per M8 screw is calculated as 44680.43 N in Section 3.13. and with the sixteen M8 screws maximum possible preload is equal to 714886.88 N. Preload from M8

tightening screws is still 332310.67 N less than the preload from M10 screws even with the increment in the number. The other drawback of going to the smaller size of the tightening screw is to have relatively early plastic deformation of micro-asperities.

The other possibility is to go for the M12 tightening screw, let us calculate the maximum possible preload from M12 screws. Keeping the clearance of 1.45 mm, the same as for M10 screws, the number of possible M12 bolts is ten, and the preload per M12 screw is calculated as 150796.45 N in Section 3.13. The maximum possible preload by using M12 is equal to 1507964.5 N which is 460766.95 N higher than from M10 screws. Also, by using M12 screws a delay can be achieved in the plastic deformation of micro-asperities.

The same trend can be observed in the Ø50 mm pin system by replacing the M10 screws with M12 screws as well as, by reducing the number of tightening screws for conical sleeves.

6.6 Errors in the results from the experiment

For Ø50 mm pin system the values of measured strain are used only from strain gauge 1 as the values from strain gauge 2 were almost half of the calculated values which might be due to human error while soldering the wires. For Ø80 mm pin system, average values from both strain gauges are used. Table 6.7 and Table 6.8 are showing the values and errors between the measured values and calculated values for Ø50 mm pin system and Ø80 mm pin system respectively. The average error for Ø50 mm pin system is -10.74% and for Ø80 mm pin system it is 8.71%.

Table 6.7: Error between measured and calculated values for Ø50 mm pin system

Applied torque	Calculated strain	Measured strain	Error
Nm	µm/m	µm/m	%
0	0	0	0
40	377.23	368.4	2.34
60	565.85	608.8	-7.59
80	754.46	873.12	-15.73
100	943.08	1104	-17.06
120	1131.69	1366	-20.70
140	1320.31	1537.7	-16.47

Table 6.8: Error between measured and calculated values for Ø80 mm pin system

Applied torque	Calculated strain	Measured strain	Error
Nm	µm/m	µm/m	%
0	0	0	0.00
40	252.61	221.5	8.95
60	378.91	311.5	15.55
80	505.22	416	13.30
100	631.52	585	2.77
120	757.83	676	9.74
140	884.13	789.5	10.65

Possible reasons for errors in experimental values are:

- For theoretical calculations and Finite Element Analysis, the central pin is assumed to have a constant cross-sectional area whereas, practically the central pin has a chamfer on both sides as well as it has threads on both ends
- Due to circular surface, it is quite challenging to position the strain gauge exactly at 90-degree angle which can also cause an error in readings
- While the application of strain gauges it is a challenging task to paste strain gauge after inserting the central pin in the test jig because of limited available space. The solution for that was to cut the wires of strain gauge and resolder them which might affect the accuracy of results
- While the application of torque, a fixture (shown in Figure 6.10) was used with torque wrench which might have absorbed a little bit of torque.



Figure 6.10: Fixture used with torque wrench

7 Conclusion

The bondura® pin system is in the initial design phase where it is important to analyze different prospects and this thesis is an addition to the process of analyzing and verifying the different properties. One of the major focus of this thesis is to analyze the different factors that go under consideration for the maximum possible preloads from the bondura® pin system and the relationship between applied torque level and preload as well as, the possible wedge effect from the conical sleeves.

And the other part of this thesis focused on the comparison between bondura® pin system and standard bolts in terms of preload capability, loss in preload due to plastic deformation of micro-asperities, and surface resistance between mating surfaces. To fulfill the purposes of this thesis, three forms of analysis, theoretical, experimental, and finite element analysis, are performed throughout the semester.

The bondura® pin system uses the tightening screws with the strength class of 16.9 so, the only possibility to improve the preload capability is either by increasing the number or the size of tightening screws. With the increment of the number of tightening screws, the geometrical properties have to be altered but with the increment of size of tightening screw only the threaded holes in the coned nuts are required to change. By increasing the tightening screw to M12 there is a significant improvement of 460766.95 N in the preload.

In the design process, it is important to verify the calculated results with the experimental results, which is achieved in this thesis for preload in both bondura® pin systems at different levels of applied torque. Also with the availability of modern means, the stress distribution for both pin systems is simulated on the ANSYS, which shows promising results for the possibilities of having much more preload without the failure.

To make a final statement on the wedge effect from the conical sleeves might be premature at this stage as this needs further study which was not in the scope of this thesis but from the results in this thesis, it can be concluded that the wedge effect from the conical sleeves provides more preload in the central pin rather than making it to lose the preload.

In comparison with the standard bolts, even though in terms of maximum possible preload capability the bondura® pin system is less capable than standard bolts, but it does provide the good surface resistance due to the much higher mating surface area. When the major concern is avoiding any radial and rotational movements bondura® pin system is the better option. The other best possible solution is to use both bondura® pin systems and standard bolts in an optimized manner.

In comparison with the big size standard bolts, the existing design of the bondura® pin system uses M10 size of tightening screws, and micro-asperities in these relatively smaller screws tend to go under plastic deformation earlier than bigger bolts.

Bondura® pin system has very much potential to solve the complicated common problems of the industry but it needs some more experimentations and improvements in terms of preload capability and optimization. Future work is recommended.

7.1 Future work recommendations

There are few points to further investigate about this design of bondura® pin system

- Developing a mathematical model for the optimization of standard bolts and bondura® pin systems
- Effect of introducing a simple nut on one side of the bondura® pin system instead of having M10 bolts and nut plate
- From the wedge effect of the conical sleeve, there is a reaction force R_3 as shown in Figure 3.2, which is being applied on the nut plate instead of the flange body. It would be interesting to further investigate that by applying more torque on M10x60 bolts (means increasing R_3) would that reduce the preload in the central pin.

8 References

- [1] «Bondura AS,» bondura technology, [Internett]. Available: <https://bondura.no/om-oss/our-history/>.
- [2] J. L. M. a. L. G. Kraige, Engineering Mechanics Statics, 7th Edition, John Wiley & Sons, Inc..
- [3] H. R. B. a. G. H. S. Jack A. Collins, Mechanical Design of Machine Elements and Machines: A failure Prevention Perspective, Second Edition, John Wiley and Sons Inc., 2010.
- [4] J. K. N. Richard G. Budynas, Shigley's Mechanical Engineering Design, McGraw Hill Education, 2015.
- [5] D. M. B. F. E. N. Boris M. Klebanov, Machine Elements: Life and Design, CRC Press, 2008.
- [6] E. R. J. J. J. T. D. a. D. F. M. Ferdinand P. Beer, Mechanics of Materials 6th Edition, McGraw Hill companies, 2012.
- [7] A. S. Morris, Measurement & Instrumentation Principles. 3rd Edition, 2001.
- [8] K. Hoffmann, Applying the Wheatstone Bridge Circuit, HBM company.
- [9] H. company. [Internett]. Available: <https://www.hbm.com/en/0364/strain-gauges-for-stress-analysis/>.
- [10] U. company, «TORQUE WRENCHES WITH REVERSIBLE RATCHET,» [Internett].
] Available:
<https://www.usag.it/catalog/en/products/pdf/2309/Torque%20wrenches%20with%20reversible%20ratchet.pdf>.
- [11] ASME, «Guidelines for Pressure Boundary Bolted Flange Joint Assembly». USA
] Patentnr. ASME PCC-1–2010, 2010.
- [12] A. A. Luiz Otavio, Machinery Failure Analysis Handbook: Sustain your operations and
] maximize uptime, 2006.
- [13] R. J. S. Arthur P. Boresi, Advanced Mechanics of Materials, Sixth edition, John Wiley &
] Sons, Inc., 2003.

[14 R. A. F. Hugh D. Young, University Physics with Modren Physics, Addison Wesley, 2012.
]

9 Appendix

9.1 Appendix A: Material properties of the central pin

Table 9.1: Material properties of the central pin

Basic thermal	
Thermal conductivity	1.872E-04 btu/(in.sec.°F)
Specific heat	.0105 btu/(lb.°F)
Thermal exp. Coefficient	6.111E-06 inv°F
Mechanical	
Behavior	Isotropic
Young's Modulus	3.046E+07 psi
Poisson's ratio	0.28
Shear modulus	1.450E-03 psi
Density	
Strength	
Yield strength	1.45E+05 psi
Tensile strength	1.740E+05 psi

9.2 Appendix B: Certificate of Strain gauges

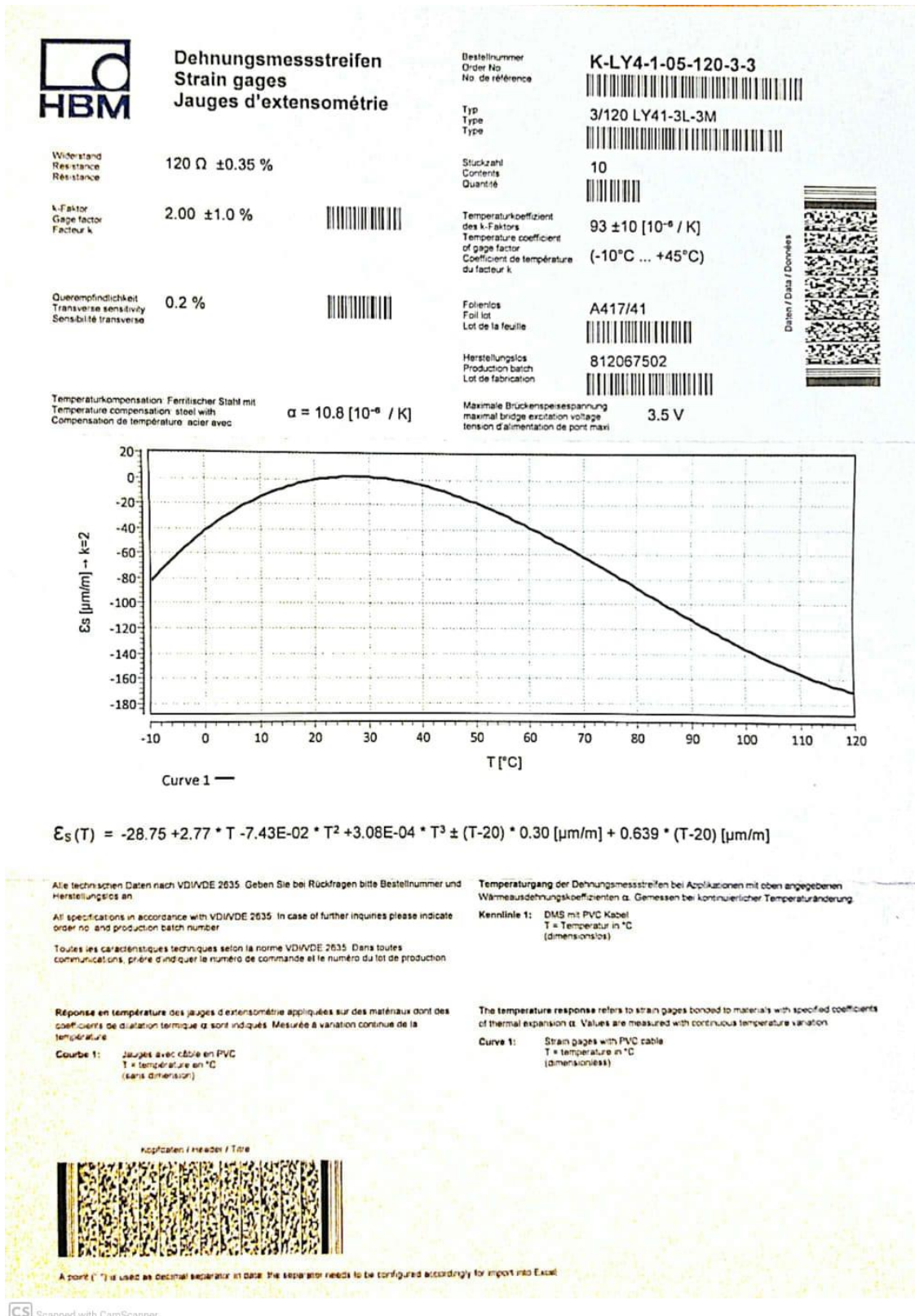



Figure 9.1: Certificate for strain gauges

9.3 Appendix C: Calibration certificate of torque wrench



REPORT DI TARATURA

CALIBRATION TEST REPORT

Nr.: F022009000728

STRUMENTO VERIFICATO
TESTED INSTRUMENT

Descrizione dello strumento : Chiave dinamometrica a scatto
Torque instrument description

Marca : USAG
Brand

Articolo : 810 N 200
Item number

Capacità : 40 a 200 N.m
Torque range

Numero di serie : H2110873
Serial number

Coppia impostata (Nm) <i>Selected torque value N.m</i>	Valori di coppia rilevati (Nm) <i>Found torque values N.m</i>	
	Senso di applicazione "Destro" <i>Torque application: clockwise</i>	Senso di applicazione "Sinistro" <i>Torque application: counterclockwise</i>
40	41,21	---
120	123,87	---
200	204,02	---

Strumento utilizzato per la taratura : CC-400 CS-5 N° P4944-8 400 N.m
Calibration device


Norma di riferimento : in conformità alle prescrizioni della norma ISO 6789 in vigore
Calibration procedure: in conformity with the specifications of in use ISO 6789 standard

Tipo e Classe dello strumento : Tipo "II" - Classe "A"
Type & Class of torque instrument

Tolleranze (Norma ISO 6789): ± 4 %
Permissible deviation (ISO 6789 Standard)

Data verifica taratura : 02/02/2009
Calibration date


Taratura effettuata da : EDA SILVA
Calibration responsible

Responsabile Centro di Taratura "U.A. S.r.l.": 
Head of the Calibration Centre

Data di acquisto / Purchasing date

Data / Purchase / Date of acquisition
Data / Date / Seller approval

SWK Utensilerie S.r.l.
Sede legale: Piazza Meda, 3 - 20121 Milano
Sede operativa: Via Volta, 3 - 21020 Monvalle (VA) - ITALIA
Tel.: +39 0332 790111 Fax: +39 0332 790602
http://www.usag.it e-mail: info.ny@usag.it



mod. EMV.SMQ.060b

Figure 9.2: Calibration certificate of torque wrench

9.4 Appendix D: Drawings of bondura® pin systems

Figure 8.3 is showing the drawing of Ø50 mm pin system and Figure 8.4 is showing the drawing of Ø80 mm pin system

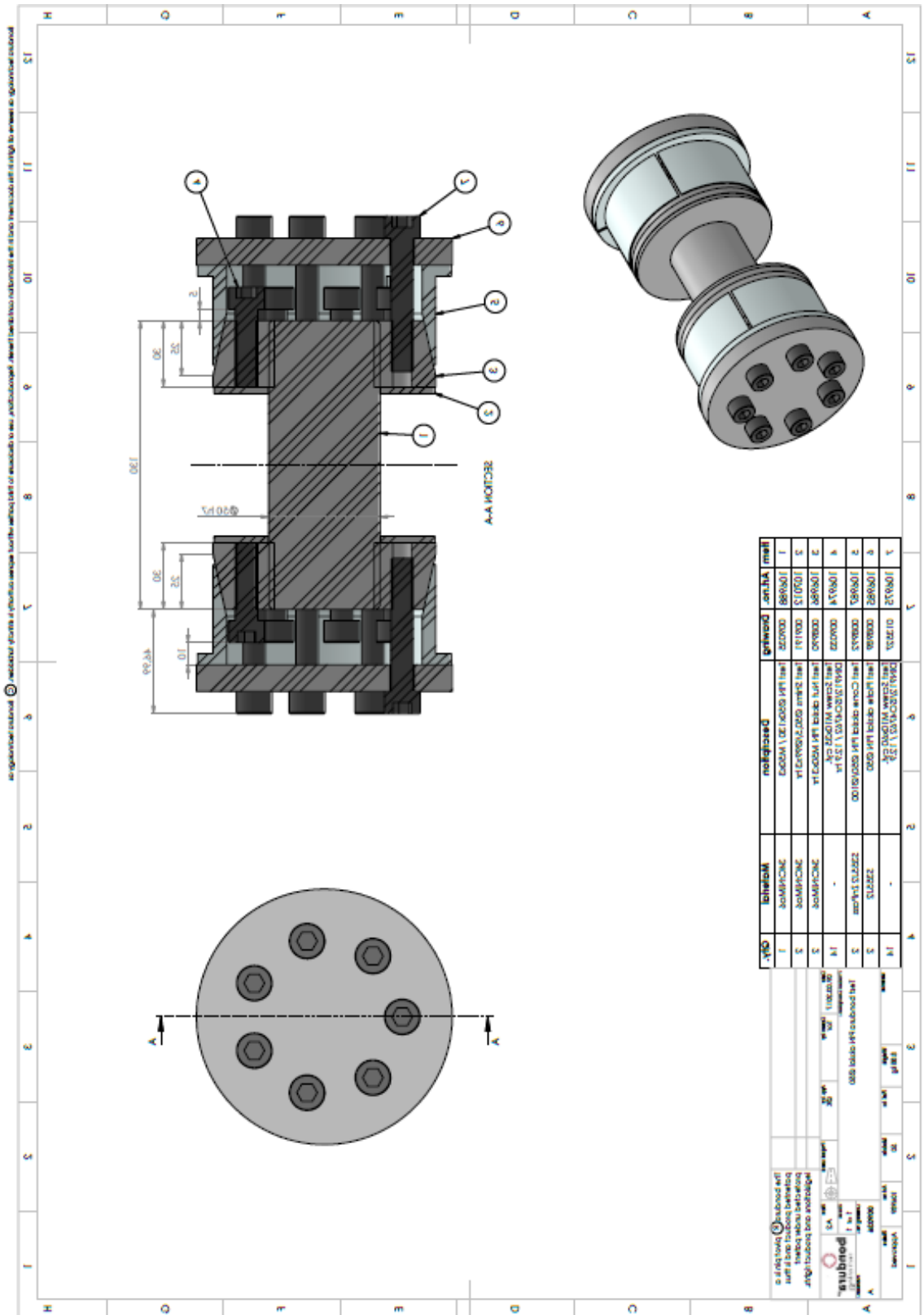


Figure 9.3: Drawing for Ø50 mm pin system

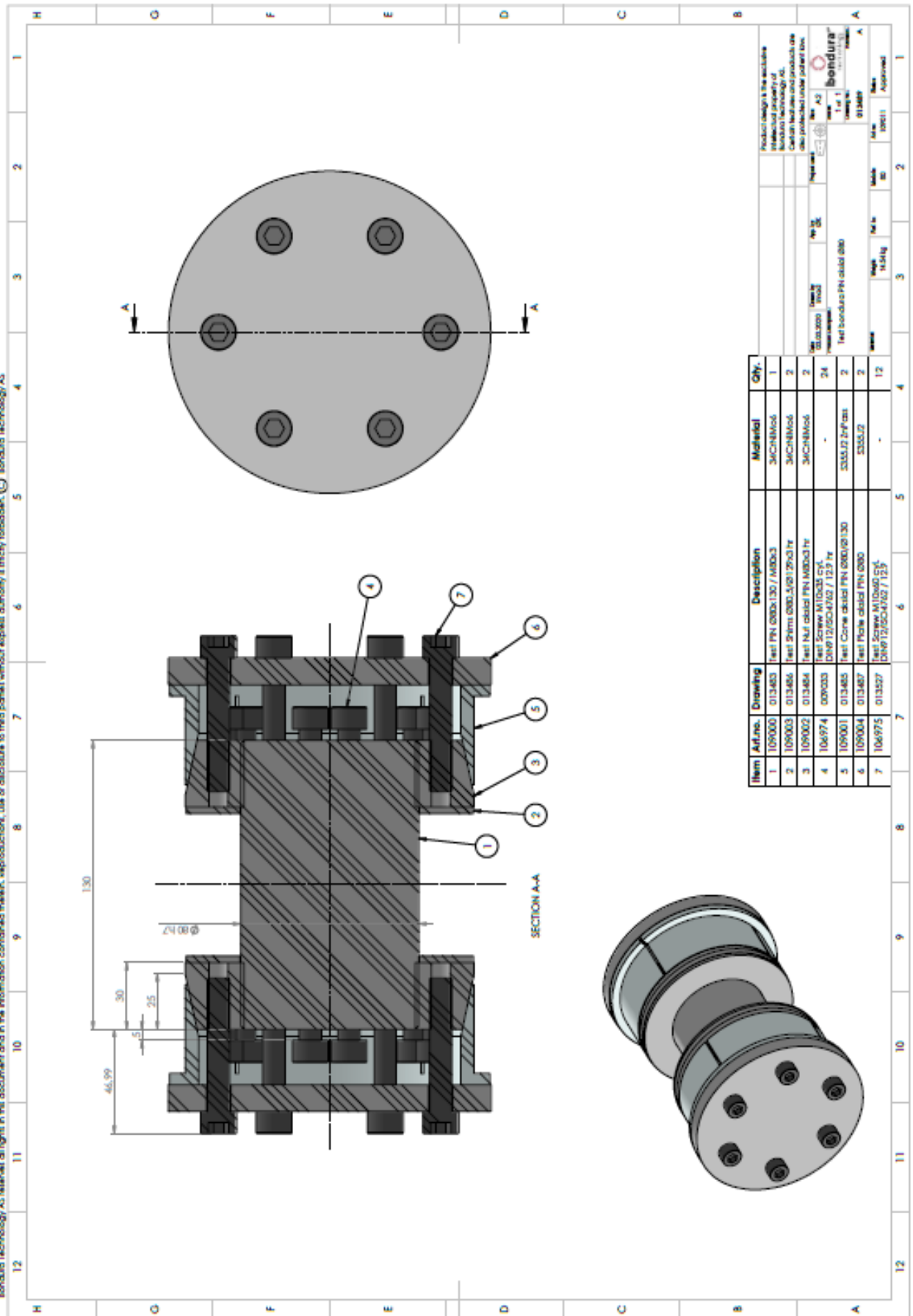


Figure 9.4: Drawing for Ø80 mm pin system

9.5 Appendix E: Stress distribution in Ø50 mm pin system at different levels of torque

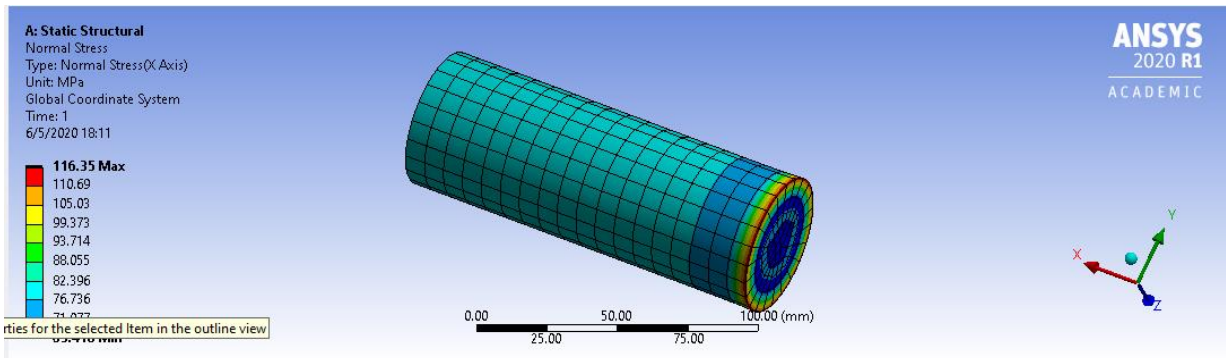


Figure 9.5: Stress distribution at 40 Nm torque in Ø50 mm pin system

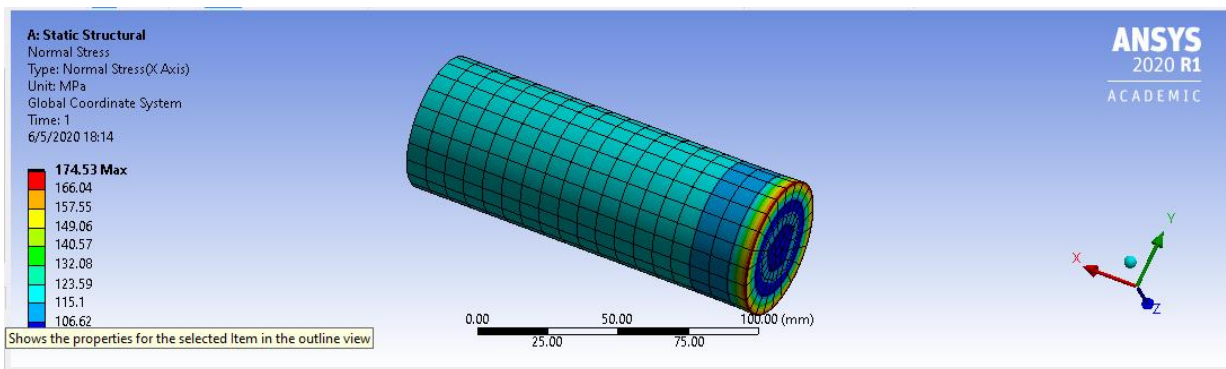


Figure 9.6: Stress distribution at 60 Nm torque in Ø50 mm pin system

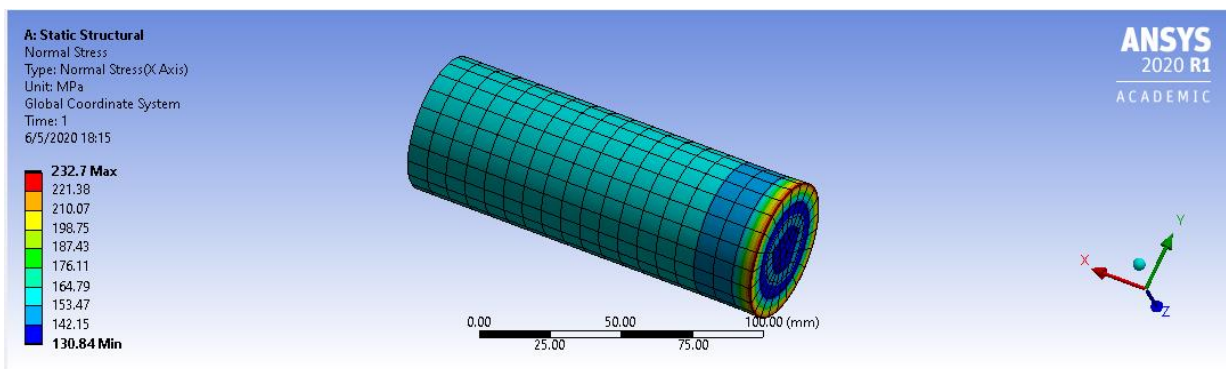


Figure 9.7: Stress distribution at 80 Nm torque in Ø50 mm pin system

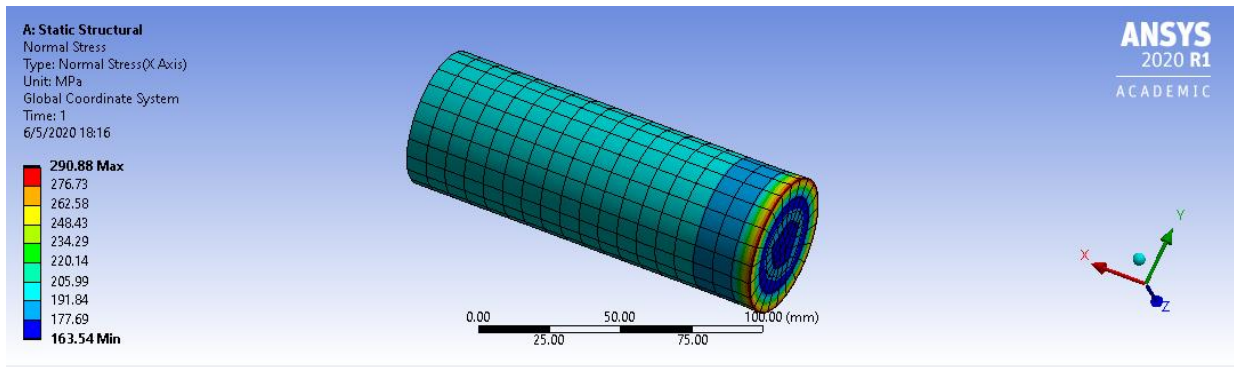


Figure 9.8: Stress distribution at 100 Nm torque in Ø50 mm pin system

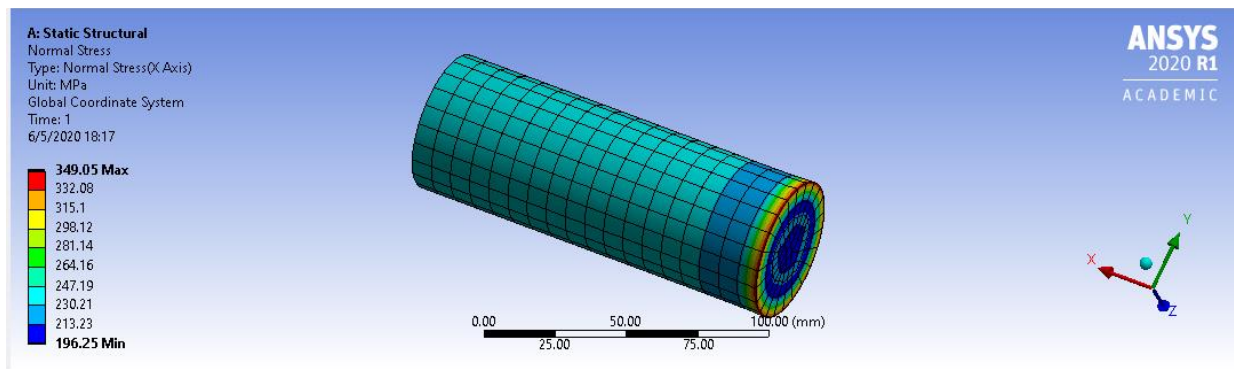


Figure 9.9: Stress distribution at 120 Nm torque in Ø50 mm pin system

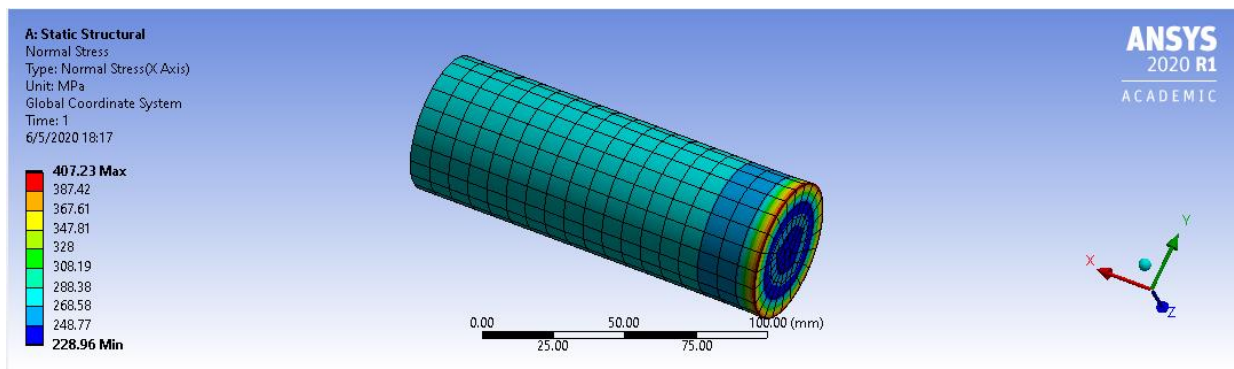


Figure 9.10: Stress distribution at 140 Nm torque in Ø50 mm pin system

9.6 Appendix F: Stress distribution in Ø80 mm pin system at different levels of torque

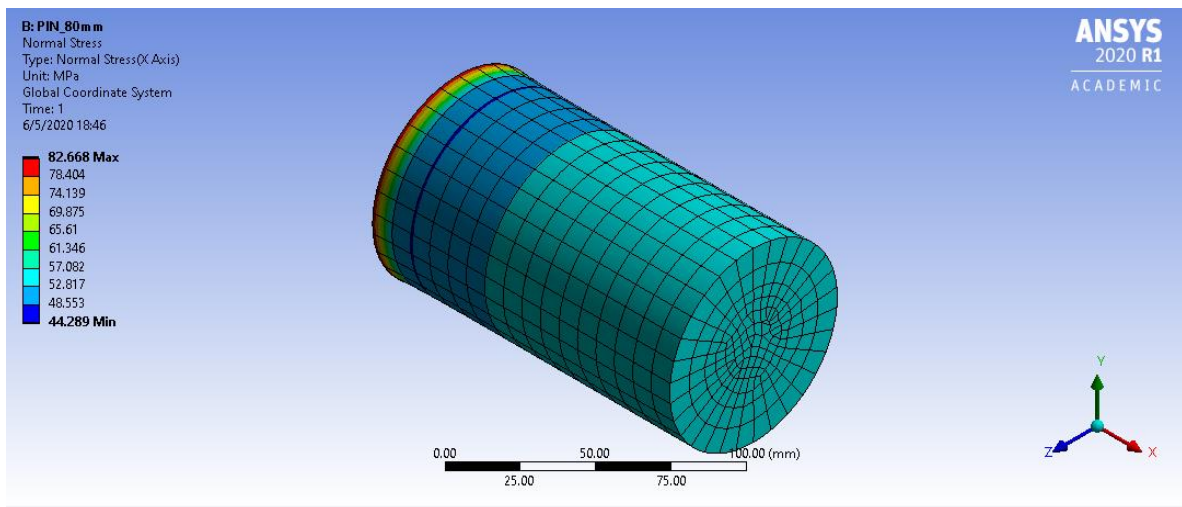


Figure 9.11: Stress distribution at 40 Nm torque in Ø80 mm pin system

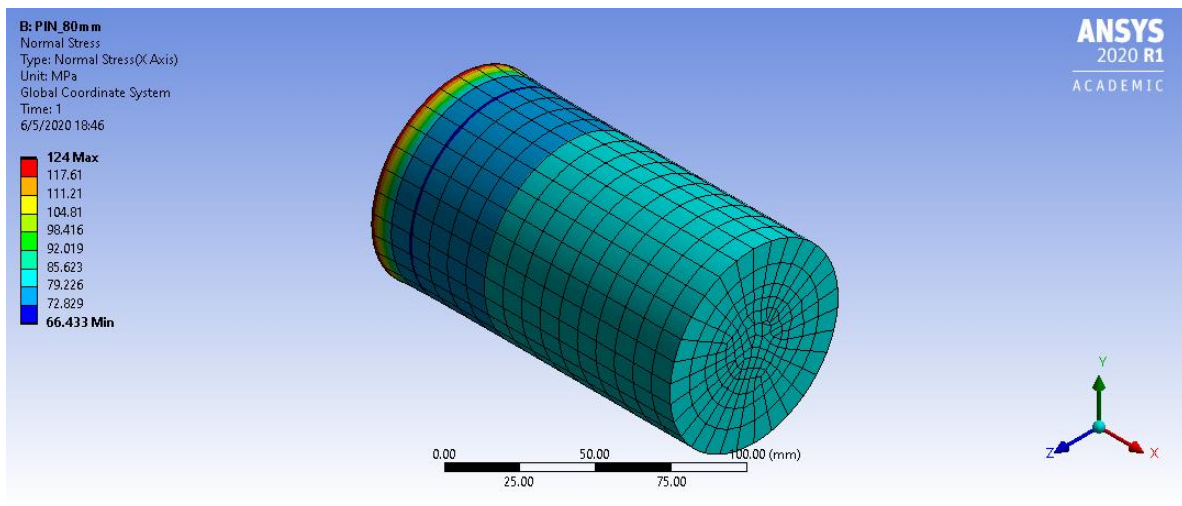


Figure 9.12: Stress distribution at 60 Nm torque in Ø80 mm pin system

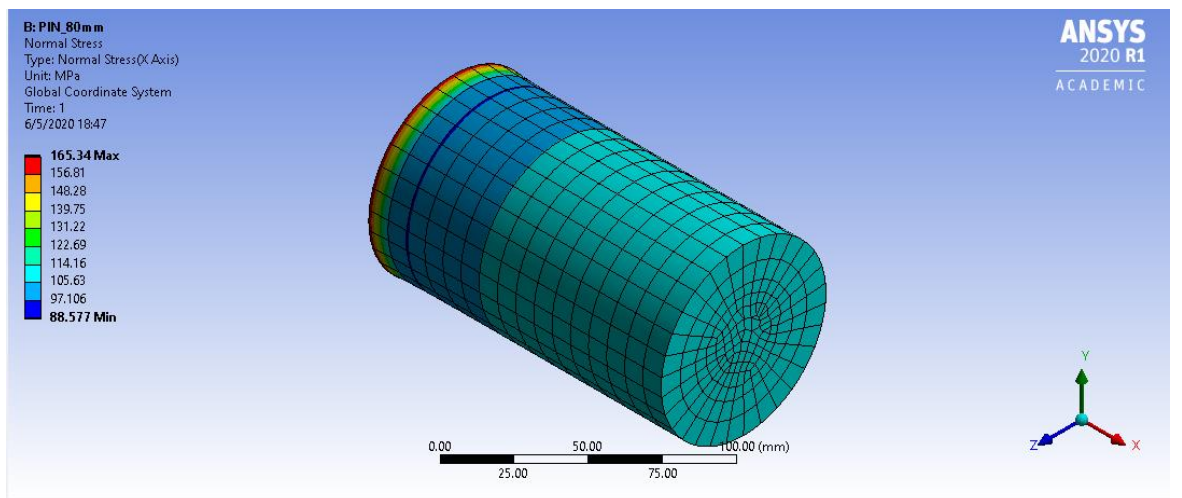


Figure 9.13: Stress distribution at 80 Nm torque in Ø80 mm pin system

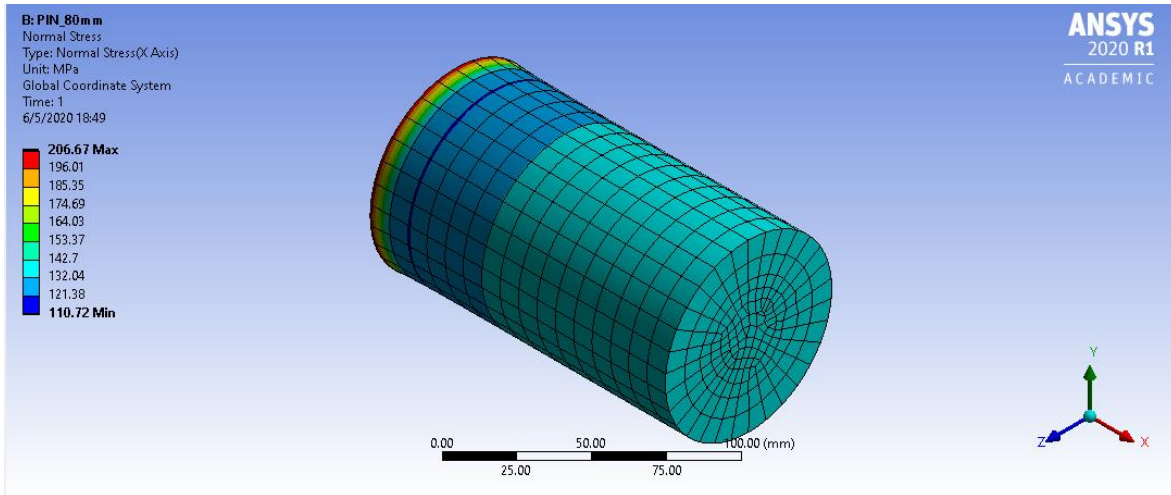


Figure 9.14: Stress distribution at 100 Nm torque in Ø80 mm pin system

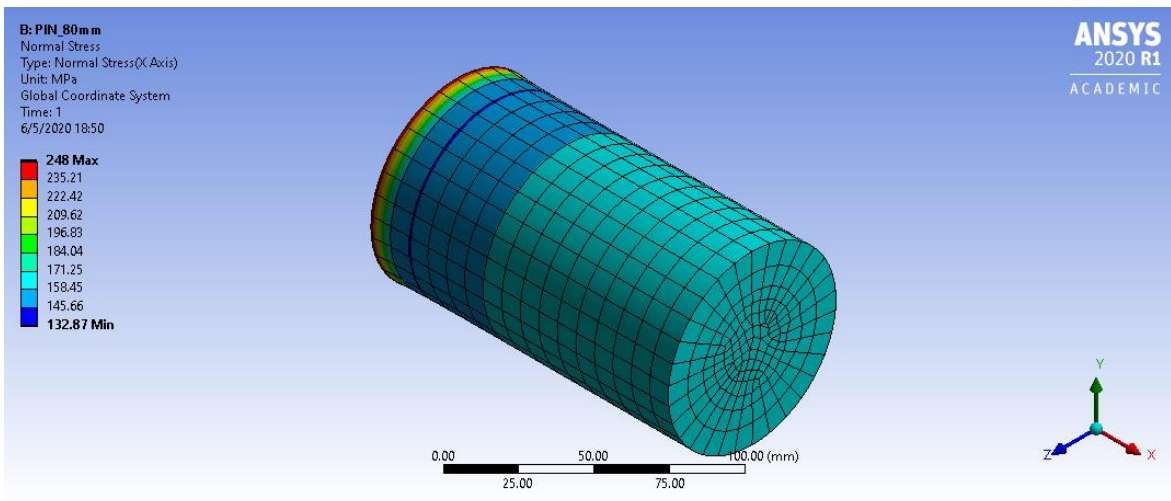


Figure 9.15: Stress distribution at 120 Nm torque in Ø80 mm pin system

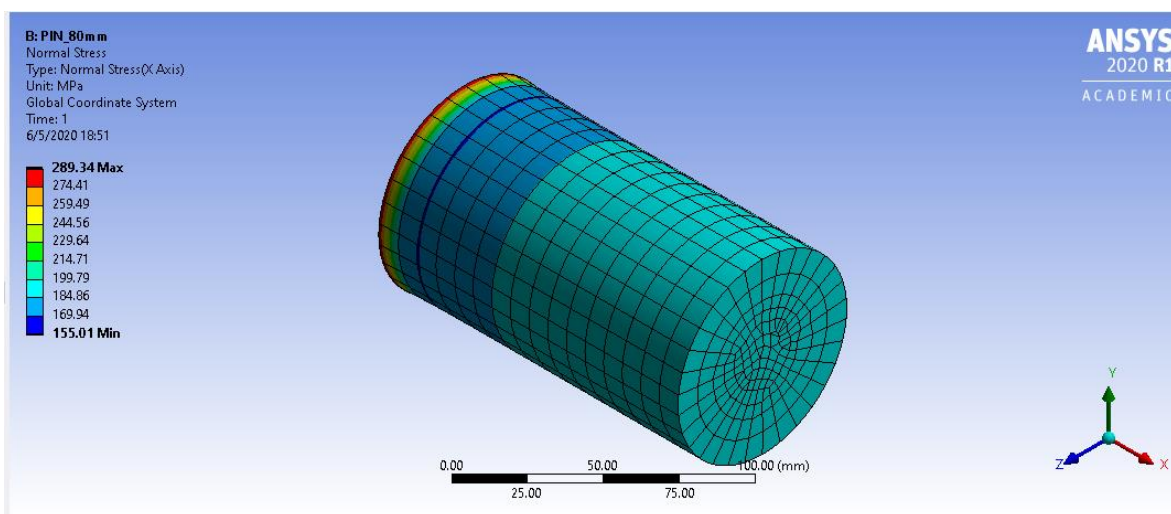


Figure 9.16: Stress distribution at 140 Nm torque in Ø80 mm pin system

Loss in preload due to plastic deformation of micro-asperities											
Compliance of bolt	Diameter of bolt, d	Elastic modulus of bolt, Eb	Compliance of thread	height of bolt head, h	Compliance of bolt head	Length of shank, L	Cross-sectional	Compliance of bolt shank	Total compliance of bolt		
	mm	MPa	mm/N	mm	mm/N	mm	mm ²	mm/N	mm/N		
	M10	10	2.06E+05	4.13E-07	10	7.28E-08	30	78.54	1.85E-06	2.34E-06	
	M50	50		8.25E-08	35	2.08E-08	60	1963.50	1.48E-07	2.52E-07	
M80	80		5.16E-08	51	1.43E-08	60	5026.55	5.79E-08	1.24E-07		
Compliance of flanges	Diameter of bolt	Major diameter of bolt, d0	Tangent of cone of pressure angle	Elastic modulus of flange, Ef	Compliance of flange						
	mm	mm		MPa	mm/N						
	M10	16	11	0.5	2.06E+05	5.31E-07					
	M50	83	53			5.76E-08					
M80	115	83			3.87E-08						
Elastic elongation	Preload, Fi	Elastic elongation	Elastic elongation of flange	Total elastic deformation							
	N	mm	mm	µm							
	M10	87266.46	0.204	0.0463	250.49						
	M50	2181662	0.549	0.1256	674.69						
M80	5585054	0.691	0.2164	907.83							
Reduction in preload	Mean height of microasperities	Pairs of contacting surfaces	Deformation of Plasticity	Decrease in elastic deformation	Ratio of reduction of initial elastic deformation	Decrement in preload					
	µm			µm		N					
	M10	5	3	1/3	10.00	0.0399	3483.89				
	M50		4		13.33	0.0198	43114.35				
M80		4		13.33	0.0147	82027.69					
Effects on initial preload	Remaining Preload	PIN size		Total loss in Preload	Remaining Preload						
	N			N	N						
	M10	83782.57	Ø50 mm pin system		24387.26	586477.98					
	M50	2138547.22	Ø80 mm pin system		41806.73	1005390.82					
M80	5503025.91										

Figure 9.19: Calculations for loss in preload for bondura® pin systems and standard bolts

Wedge effect of the conical sleeve											
Mass calculation		mp	mshim	mnut	mb1	mplate	mb2	friction coefficient	φ	α	mass
		kg	kg	kg	kg	kg	kg				
	Ø50 mm pin system	1.99	0.13	1.12	0.031	0.91	0.0465	0.6	0.540	0.209	3.70
Ø80 mm pin system	5.09	0.19	1.57	0.031	1.49	0.0465	0.6	0.540	0.209	6.45	
Reaction forces		weight	applied torque	applied forced	R2	R3					
		N	Nm	N	N	N					
	Ø50 mm pin system	36.27	70	35000	51378.87	51378.86					
Ø80 mm pin system	63.24	70	35000	51378.87	51378.83						
Effects of wedge		Previous load on pin	Total load	Area	Stress	Strain					
		N	N	mm ²	MPa	microm/m					
	Ø50 mm pin system	610865.24	662244.09	1963.50	337.28	1605.98					
Ø80 mm pin system	1047197.55	1098576.38	5026.55	218.55	1040.67						
Effect on initial stress		Previous stress	Extra stress								
		MPa	MPa								
	Ø50 mm pin system	311.11	26.17								
Ø80 mm pin system	208.33	10.22									

Figure 9.20: Wedge calculations for conical sleeves

Preload calculations for Standard bolt							
	Diameter	Radius	Polar moment of inertia	Experimental factor			
	mm	mm	mm ⁴				
M50	50	25	613592.32	0.18			
M80	80	40	4021238.60				
				Maximum Torque		Maximum preload	
Bolt strenght class	Tensile Strength	Yield strength	Maximum shear stress	M50	M80	M50	M80
	MPa	MPa	MPa	Nmm	Nmm	N	N
8.8	800	640	400	9817477.04	40212385.97	1090830.78	2792526.80
10.9	1000	900	500	12271846.30	50265482.46	1363538.48	3490658.50
12.9	1200	1080	600	14726215.56	60318578.95	1636246.17	4188790.20
16.9	1600	1440	800	19634954.08	80424771.93	2181661.56	5585053.61

Figure 9.21: Preload calculations for standard bolts

Surface areas								
Standard bolts				Bondura® pin system				
		M50	M80			50 mm	80 mm	
Diameter of bolt head	mm	83	115		Width of sleeve in contact	mm	23.24	23.24
Diameter of bolt	mm	50	80		Radius of conical sleeve	mm	50	65
Diameter of nut	mm	83	115		Contact area without slots	mm ²	7301.06	9491.38
Contact surface area	mm ²	6894.23	10720.68		Slots area	mm ²	46.48	46.48
					Contact area with slots	mm ²	14230.28	18610.92
					Outer diameter of shims	mm	99	129
					Inner diameter of shims	mm	50.5	80.5
					Area of shims	mm ²	11389.45	15960.47
					Total contact surface area	mm ²	25619.73	34571.39

Figure 9.22: Calculations for mating surface area of both type of fasteners